

cy.6



**MEASUREMENT OF POLLUTANT EMISSIONS  
FROM AN AFTERBURNING TURBOJET ENGINE  
AT GROUND LEVEL  
PART I. PARTICULATE EMISSIONS**

**J. W. Gearhart and J. A. Benek  
ARO, Inc.**

**June 1972**

Approved for public release; distribution unlimited.

**ENGINE TEST FACILITY  
ARNOLD ENGINEERING DEVELOPMENT CENTER  
AIR FORCE SYSTEMS COMMAND  
ARNOLD AIR FORCE STATION, TENNESSEE**

# ***NOTICES***

When U. S. Government drawings specifications, or other data are used for any purpose other than a definitely related Government procurement operation, the Government thereby incurs no responsibility nor any obligation whatsoever, and the fact that the Government may have formulated, furnished, or in any way supplied the said drawings, specifications, or other data, is not to be regarded by implication or otherwise, or in any manner licensing the holder or any other person or corporation, or conveying any rights or permission to manufacture, use, or sell any patented invention that may in any way be related thereto.

Qualified users may obtain copies of this report from the Defense Documentation Center.

References to named commercial products in this report are not to be considered in any sense as an endorsement of the product by the United States Air Force or the Government.

**MEASUREMENT OF POLLUTANT EMISSIONS  
FROM AN AFTERBURNING TURBOJET ENGINE  
AT GROUND LEVEL  
PART I. PARTICULATE EMISSIONS**

**J. W. Gearhart and J. A. Benek  
ARO, Inc.**

Approved for public release; distribution unlimited.

## FOREWORD

The test program reported herein was conducted at the request of the Air Force Aero Propulsion Laboratory (AFAPL), Air Force Systems Command (AFSC), Wright-Patterson Air Force Base, Ohio, under AFAPL Project Orders 71-7 and 72-9, Project 3066. The AFAPL Project Engineer was Mr. K. N. Hopkins, and the AEDC Air Force Program Monitor was Mr. E. L. Hively. The test hardware, support hardware, test planning, and test procedures, exclusive of the J85-GE-5 turbojet engine and a mobile control van, were provided by AEDC. The turbojet engine and mobile control van were supplied by AFAPL.

The results of the test program were obtained by ARO, Inc. (a subsidiary of Sverdrup & Parcel and Associates, Inc.), contract operator of the Arnold Engineering Development Center (AEDC), AFSC, Arnold Air Force Station, Tennessee, under Contract F40600-72-C-0003. The test was conducted at the Ground Level Test Stand of the Engine Test Facility (ETF) during the period from March 23 to May 13, 1971, under ARO Project Nos. RW5139 and RW5239. The manuscript was submitted for publication on March 20, 1972.

This report presents the results from the first part of a two-part test program and describes the measurement of smoke emissions from an afterburning turbojet engine. The results of the second part are presented in AEDC-TR-72-70 which describes a portable system for measuring gaseous emissions from an afterburning turbojet engine.

This technical report has been reviewed and is approved.

EULES L. HIVELY  
Research and Development  
Division  
Directorate of Technology

R. O. DIETZ  
Acting Director  
Directorate of Technology

**ABSTRACT**

Smoke emissions were measured in general accordance with the methods specified in the Society of Automotive Engineers Aerospace Recommended Practice 1179. Measurements were made from 1 in. to 32 ft aft of the nozzle exit along the engine centerline, and both horizontally and vertically across the exhaust plume. The J85-GE-5 turbojet engine was operated over a power range from idle to maximum afterburning. The effects of inlet temperature and humidity on smoke production were determined, and trends of smoke production versus power setting were established.

## CONTENTS

	<u>Page</u>
ABSTRACT . . . . .	iii
NOMENCLATURE . . . . .	vi
I. INTRODUCTION . . . . .	1
II. APPARATUS . . . . .	1
III. PROCEDURE . . . . .	3
IV. RESULTS AND DISCUSSION . . . . .	4
V. SUMMARY OF RESULTS . . . . .	8
REFERENCES . . . . .	9

## APPENDIXES

## I. ILLUSTRATIONS

Figure

1. Schematic of Smoke Sampling System . . . . .	13
2. J85-GE-5 Turbojet Engine	
a. Cutaway Section . . . . .	14
b. Photograph . . . . .	14
3. Exhaust Nozzle Area versus Power Lever Angle . . . . .	15
4. Ground Level Test Stand	
a. Schematic . . . . .	16
b. Photograph . . . . .	17
5. Variation on Centerline	
a. SN, 1 ft Aft, Cruise . . . . .	18
b. SN, 2 ft Aft, Military . . . . .	19
c. SNR, at the Nozzle Exit, Cruise . . . . .	20
6. Centerline Smoke Values as a Function of Distance . . . . .	21
7. SNR Profile at Nozzle Exit	
a. Military Power . . . . .	22
b. Cruise Power . . . . .	23
c. Idle Power . . . . .	23
8. Radial Profiles on SNR (View Looking Upstream)	
a. 1 ft Aft of Nozzle Exit . . . . .	24
b. 4 ft Aft of Nozzle Exit . . . . .	25
c. 16 ft Aft of Nozzle Exit . . . . .	26
9. Effects of Distance on SNR Profiles at Military Power (View Looking Upstream) . . . . .	27
10. Effect of Power Level at 16 ft Aft of the Nozzle Exit on the Engine Centerline	
a. On SNR Values . . . . .	28
b. On Filters—Photograph . . . . .	28
11. Profiles of Exhaust Total Pressure at the Nozzle Exit, Military Power . . . . .	29

<u>Figure</u>	<u>Page</u>
12. Profiles of Exhaust Total Pressure at 16 ft Aft of the Nozzle Exit at Various Power Levels . . . . .	30
13. SNR Profiles at Afterburner Power, 16 ft Aft of the Nozzle Exit . . . . .	31
 II. TABLES	
I. Engine Operation Parameters at	
$P_{inlet} = 14.2$ psia, $T_{inlet} = 59^{\circ}\text{F}$ . . . . .	32
II. Chemical Composition of JP-4 Fuel . . . . .	33
III. METHOD OF DATA REDUCTION . . . . .	34
IV. A TECHNIQUE FOR THE REDUCTION OF SMOKE NUMBER DATA . . . . .	37

**NOMENCLATURE**

A	Gas flow area, generally taken to be equal to $A_t$
$A_p$	Area covered by the particles deposited on the filter paper
$A_t$	Total area of filter paper exposed to the particles
$C_1$	$a_o / \nu_1 \rho \Delta t$
$C_2$	$\beta C_1$
$E_o$	Total incident energy
$E_r$	Total error in measured SN
$e_1$	Error in $R_S$ measurement
$e_2$	Error in $R_W$ measurement
$K_1$	$C_1 n_{p\infty}$
$K_2$	$C_2 n_{p\infty}$
$n_{ps}$	Number of particles deposited on the filter paper surface
$n_{p\infty}$	Free-stream or ambient particle number density
$R_S$	Reflectance of partially covered filter paper
$R_W$	Reflectance of clean filter paper
SN	Smoke number

SNR	Relative smoke number
W	Total mass flow through the filter paper
a	Probability that a particle sticks to the filter surface and changes the area covered by the particles
a <sub>0</sub>	“Sticking” probability of a particle on a clean filter surface
a <sub>1</sub>	Absorbptivity of the particles
a <sub>2</sub>	Absorbptivity of the filter paper
β	$100 \left[ \frac{\epsilon_1 - \epsilon_2}{(E_0/A_1) - \epsilon_2} \right]$
γ	A constant
ε <sub>1</sub>	Energy absorbed per unit particle area
ε <sub>2</sub>	Energy per unit area absorbed by the clean filter paper
θ	The fraction of the total filter surface area covered by particles
μ	Strike rate or collision rate of particles with the filter surface
ν	Rate at which particles are effectually “knocked off” the filter surface causing a change in the area covered by the particles

#### SUBSCRIPTS

Q	Centerline point
m	Measured values of quality

## SECTION I INTRODUCTION

Because of the increasing utilization of gas turbine engines and the growing concern over the effects of the exhaust products of these engines on the atmosphere, several investigations of the production of solid pollutants by turbine engines have been made (Refs. 1 and 2). However, very little information is available in the literature describing the pollutant production of afterburning engines. In this report are described the results of a test program concerned with the evaluation of instrumentation and measurement of smoke produced by a turbojet engine at both normal and afterburning power levels.

This work was part of an overall program to develop and test a portable, easy to operate, pollution measurement system for the Air Force Aero Propulsion Laboratory. Instrumentation to measure both gaseous and particulate pollutants was installed in a trailer. Gaseous species which may be measured and recorded continuously are carbon monoxide (CO), carbon dioxide (CO<sub>2</sub>), total hydrocarbons (C<sub>x</sub>H<sub>y</sub> measured as CH<sub>4</sub> equivalent), nitrogen dioxide (NO<sub>2</sub>), and total oxides of nitrogen (NO<sub>x</sub>). A description of the measurement systems for the gaseous species and the typical performance of these systems are contained in Ref. 3.

Particulate measurements were made in general accordance with SAE Aerospace Recommended Practice (ARP) No. 1179 (Ref. 4). Other applications of the recommendations in ARP 1179 are described in Refs. 5 and 6.

The exhaust from a J85-GE-5 turbojet engine (Ref. 7) was sampled at various operating conditions of the engine, including afterburner modes, and at various axial and radial positions in the exhaust plume. The J85 series engine is used in several aircraft including the Ryan XV-5A, the Northrop T-38A, the Northrop F5A, B and E, the Fiat G91V, and the Cessna A37A (Ref. 8). Performance of the measurement system and typical results of the smoke emissions from an afterburning turbojet engine are presented herein. A brief description of the measurement system utilized is given. An analysis of the measurement technique recommended in SAE ARP 1179 is also presented.

## SECTION II APPARATUS

### 2.1 SMOKE MEASUREMENT SYSTEM

Smoke measurements were made using a system fabricated in general accord with the Society of Automotive Engineers Aerospace Recommended Practice No. 1179. Samples were taken with a probe constructed of 0.370-in.-ID stainless steel tubing. The probe was attached directly to a 0.370-in.-ID, 50-ft, copper, sample line which was insulated and electrically heated to prevent condensation of water vapor and light hydrocarbons. The line was kept at about 250°F by thermostatically controlled heater tape which was wound along the copper sample line. Figure 1 (Appendix I) is a schematic of the gas flow through the filter system. Valve A was a three-way solenoid valve which directed the flow through either the filter or a filter bypass line. Valves B and C were throttle valves to control

the flow through the filter and bypass, respectively. Valve D was another three-way solenoid valve which connected the bypass and filter legs to a pump. A diaphragm-type pump was used to pull the sample gas through the filter and then push it through the flow and volume meters. A flowmeter was used for instantaneous flow measurement and control. The volume flow data were obtained from a positive displacement volume meter. Temperature and pressure were measured at the inlet of the volume meter by a thermocouple and a pressure gage to allow correction to standard temperature and pressure.

## 2.2 CALIBRATION OF THE SMOKE MEASUREMENT SYSTEM

The reflectance of the deposited spot of particulates on the filter paper was measured with a Welch Densichron 3837X reflectometer. Whatman No. 4 filter paper was used throughout the test. The diameter of the deposited spot was one-half inch. The reflectometer was calibrated as specified by Welch. All measurements were made with the filter resting on a grey tile of uniform reflectance.

## 2.3 TURBINE ENGINE

The J85-GE-5 turbojet engine (Fig. 2) has an eight-stage, axial-flow compressor directly coupled to a two-stage turbine, a through-flow annular combustor, an afterburner, and a variable-area exhaust nozzle (Ref. 7). Exhaust nozzle area is scheduled by power lever as shown in Fig. 3. The engine inlet diameter is approximately 15.4 in., and the overall length is approximately 108 in. Rated sea-level-static thrust is 2500 lbf at military power and 3850 lbf at maximum power (Ref. 7). Rated airflow is 44 lbfm/sec at 16,500-rpm compressor rotational speed. Engine operating parameters at sea-level-static conditions are shown in Table I (Appendix II).

The afterburner consists of a diffuser, a single V-gutter pilot burner which also acts as a flameholder, and a pilot burner fuel injection system. The pilot burner incorporates a spark plug igniter for afterburner ignition.

The integrated fuel system consists of main and afterburner fuel controls operated by the power lever. The main fuel control meters fuel as a function of compressor inlet total temperature, compressor discharge static pressure, engine rotor speed, and power lever angle. The afterburner fuel control houses the exhaust nozzle area control system and meters fuel to the afterburner spraybars as a function of compressor discharge static pressure and power lever angle. Nozzle area during afterburner operation is scheduled as a function of power lever angle and turbine discharge temperature.

## 2.4 INSTALLATION

The engine was mounted on an open, flat-bed trailer which was secured inside an open-ended shelter (Fig. 4) at the Ground Level Test Stand (GLTS) of the Engine Test Facility. A bellmouth was attached to the engine inlet to aid in providing uniform airflow to the engine.

The fuel for the engine was stored in a 600-gal tank located on the front of the flat-bed trailer (Fig. 4). The engine was monitored and controlled from an instrumented van which was located in front of the GLTS.

The Ground Level Test Stand includes a trapezoidal concrete slab, 100 ft in length, which was located aft of the engine nozzle exit plane (Fig. 4). The width of the slab increased from 20 ft at the nozzle exit plane to 40 ft at the 100-ft location. One of the purposes it served was to prevent entrainment of dust in the exhaust plume.

The sampling probe (Fig. 4b) was mounted on a supporting frame which was attached to the engine stand (for measurements at the tailpipe) or on a movable cart (for measurements downstream of the engine exhaust nozzle). When the probe was mounted on the engine stand, horizontal, vertical and axial adjustments were made manually. When the probe was mounted on the movable cart, axial and horizontal changes were made by moving the entire cart. Vertical straight line changes were made by a remotely controlled mechanism on the cart which allowed the probe to be traversed from 4 to 12 ft above the pad. The concrete pad was surveyed and position points marked on the pad relative to the engine centerline and exit plane. A plumb bob was used to position the probe over the desired position point. This system gave a maximum position uncertainty of about 1 in. at an axial distance of 100 ft of the tailpipe.

## **2.5 INSTRUMENTATION**

### **2.5.1 Engine Operating Parameters**

Measurements made to define engine operating conditions included engine inlet and compressor discharge total pressures, engine oil temperature, engine rotational speed, engine inlet and turbine discharge total temperatures, and engine and afterburner fuel flows. All data were manually recorded from the output of various standard gage displays in the control van, driven by standard USAF sensors.

### **2.5.2 Environmental Conditions**

A continuous recording was made of ambient temperature, relative humidity, and wind speed and direction. Atmospheric pressure was recorded on a regular two-hour schedule. Start-up of the smoke measurement system included a measurement of "ambient smoke." No measurable levels due to ambient conditions were ever observed.

## **SECTION III PROCEDURE**

### **3.1 ENGINE OPERATION**

The J85-GE-5 engine was operated at the Ground Level Test Stand (GLTS) of the Engine Test Facility (ETF). JP-4 fuel was used at all times. The specified composition of this fuel is presented in Table II. A chemical analysis of this fuel was not made; however, the fuel did test within specifications for corrosion, heating value, distillation temperatures, and specific gravity.

Typically, after start, the engine was operated at idle power for about .5 min. The engine power was then adjusted to the desired operating condition and allowed to stabilize at that condition for about 3 min until oil and exhaust gas temperatures were stable. One minute after the engine became stable, the sampling procedure was begun. After the necessary samples were taken, the engine conditions were changed, and the process was repeated. The engine was cooled between high power runs by interspersing data runs at cruise or idle between the higher power data runs or by operating at 75-percent rotor speed to provide maximum cooling. Fuel flows measured during testing were in good agreement with those specified by the manufacturer (Ref. 7) for the inlet conditions which were encountered.

### 3.2 SMOKE MEASUREMENT SYSTEM OPERATION

Several hours before beginning data acquisition, the line heater was turned on, and ambient air was drawn through the collection and filtering systems to condition them. The line was kept at approximately 250°F, and the gas temperature downstream of the filter was typically 100°F. After conditioning, the leak and cleanliness checks of the system were made as specified in Ref. 4. For all the cleanliness checks made, the values of  $R_S$  were equal to the  $R_W$  values, within measurement accuracy. After engine stabilization on condition, the system was allowed to continue flowing through the bypass loop (Fig. 4) for 1 min rather than the 5 min specified in ARP 1179 (Ref. 4) (see Section IV). The flow was then valved to the filter leg. The flow was switched back to the bypass loop when the desired gas volume had passed through the filter as indicated by the volume meter. The disk of filter paper was then removed and placed in an individual envelope, and another was clamped in place. Four different volumes were sampled at each test point, i.e., for each power setting and each axial and radial position. The volumes used were in the range recommended in ARP 1179 ( $0.00765 < W/A < 0.115$ ).

The reflectometer measurements of  $R_S$  were made within one hour of collecting the samples. Each filter disk had been measured ( $R_W$ ) before the test. The values of  $R_W$  and  $R_S$  were used to determine relative smoke number by the methods mentioned in Appendix III.

Typically,  $R_W$  values varied from 79.0 to 83.0 percent, and  $R_S$  values were observed from 66.0 to 82.5 percent.

## SECTION IV RESULTS AND DISCUSSION

The results presented herein were compiled from measurements of smoke concentration made in general accordance with ARP 1179 (Ref. 4). Measurements were made at idle; cruise; military; and minimum, intermediate, and maximum afterburner in the exhaust plume of a J85-GE-5 turbojet engine. The purpose of this test was to develop and test a portable, easy-to-operate, pollution measurement system for the Aero Propulsion Laboratory.

In Section 3.6 of ARP 1179, it is recommended that the exhaust gas be drawn through the bypass leg for 5 min after engine stabilization and only then begin to take samples. This recommendation, if followed, would have prevented the taking of any data from afterburner conditions since the engine had a limit of 5 min of continuous afterburning operation. Therefore, an investigation was made of the effects of shortening the recommended 5-min delay period. Data were taken at both cruise and military power settings, 1 min after engine stabilization, and then the data were duplicated, starting 5 min after engine stabilization. Data were taken at a constant value of W/A (Fig. 5a) and at varying values of W/A within the specified range (Fig. 5b). There was no significant difference between the 1-min delay data and the 5-min delay data for either power setting. Therefore, the shorter delay (1 min) was used for the entire study which then included afterburner data.

Variations of the SNR data from day-to-day are shown in Fig. 5c. These variations include possible wind effects, shifts of the set conditions of the engine, and the effects of changing temperature and humidity. No trends due to changes on either ambient temperature or ambient humidity were noted in the data.

The deflection produced by the greatest crosswind component noted (7 mph) would have been on the order of 1.5 in. at 16 ft aft of the nozzle exit for maximum afterburner power. For all data except that taken at idle power, the wind most probably had little effect on the plume until it was at least 16 ft downstream of the nozzle. No idle data were taken except at the nozzle exit since the direction of the exhaust gases at idle power was completely controlled by buoyancy and wind effects at a distance beyond 2 ft from the nozzle exit.

It should be noted that the J85-GE-5 engine used never produced visible smoke.

The SNR values discussed below were calculated by methods described in Appendix III.

#### 4.1 EFFECT OF DISTANCE

Centerline values of relative smoke number (SNR) were measured at various axial distances aft of the nozzle exit plane. The results are shown in Fig. 6. Afterburner data were taken only with the probe 10 ft aft of the nozzle exit or more, where the ambient conditions in the exhaust jet permitted probe survival. Idle data were taken only at the nozzle exit plane because of wind and buoyancy effects further downstream. Relative smoke number decreased monotonically as a function of axial distance for all power settings as expected with a turbulent diffusion process.

The decrease in centerline smoke intensity (SNR) (Fig. 6) was quite rapid in the first 2 ft, especially for the higher power levels. The inviscid core extended at least 2.5 diameters downstream (approximately 3 ft) at military power. Therefore, no mixing is expected in this region. This rapid decrease may be due to combustion of the carbon particles caused by higher temperatures at the higher engine power settings. The SNR values for afterburning power were generally below those produced by dry power for distances of more than 12 ft aft of the nozzle exit.

## 4.2 RADIAL PROFILES

The horizontal, radial profiles taken at the nozzle exit are shown in Fig. 7. The idle and cruise profiles were quite uniform. The military power profile was not uniform. Figure 8 shows the profiles that were taken at 1, 4, and 16 ft aft of the nozzle exit. Figures 8a and b show a definite asymmetrical SNR distribution with higher levels appearing on the left side of the centerline for all power settings. An interesting feature of this asymmetry is that it remains to the left regardless of the wind direction (Figs. 8a and b) (traverse directions were interspersed).

Relative smoke number profiles, at military power, taken at different distances downstream are shown in Fig. 9, which illustrates the smoothing and broadening of the profile due to mixing.

## 4.3 EFFECTS OF ENGINE POWER LEVEL

Plots of SNR versus engine power are shown in Fig. 10. The relative smoke number increased with nonaugmented engine power up to military power and rapidly decreased during augmented (afterburner) operation. The afterburner apparently burned the small carbon particles produced in the main engine combustors. At maximum afterburner, the SNR levels returned nearly to those produced at idle power.

Total pressure data taken at the nozzle exit and at 16 ft aft of the nozzle exit are shown in Figs. 11 and 12, respectively. It should be noted that the asymmetry observed in the SNR profiles (Fig. 8) (i.e., higher levels to the left) is seen as well in the pressure data shown in Fig. 12.

## 4.4 ERROR ANALYSIS OF THE EXPERIMENTAL MEASUREMENTS

One problem encountered in the smoke number measurements was the difficulty of accurately determining low values of relative smoke number (SNR). The profile data taken at 16 ft aft of the nozzle for afterburner power show the effect of this problem (Fig. 13). Values of SNR were low, and the data exhibited wide percentage deviation from the mean (Fig. 10). These data (Figs. 10 and 13) are of interest however since they show the generally decreasing smoke level with increasing afterburner power. Part of the problem of scatter at low smoke levels may be attributed to external influences; however, a part of the problem was also found to lie in the nature of the definition of SN (Appendix III), i.e.,

$$SN = 100 \left[ 1 - \frac{R_S}{R_W} \right] \quad (1)$$

Observe the effect of a small error in both or either of the measurements of  $R_S$  and  $R_W$ . Assume that

$$\begin{aligned} R_S &= R_{S_m} + e_1 \\ R_W &= R_{W_m} + e_2 \end{aligned} \quad (2)$$

where the subscript m refers to the measured value and  $e_1$  and  $e_2$  are the respective errors. Then,

$$SN_m = \left[ 1 - \frac{R_S + e_1}{R_W + e_2} \right] 100 \quad (3)$$

Now, since  $e_1, e_2 \ll R_W$ , the second term of Eq. (3) above can be approximated as

$$\frac{R_S + e_1}{R_W \left[ 1 + \frac{e_2}{R_W} \right]} = \frac{R_S}{R_W} + \frac{e_1}{R_W} \left[ 1 - \frac{e_2}{R_W} \right]$$

where the  $e^2$  terms have been taken to be negligible. Thus, Eq. (3) may be expressed as

$$SN_m = 100 \left[ 1 - \frac{R_S}{R_W} \right] + \frac{100 e_1}{R_W} \left[ 1 - \frac{e_2}{R_W} \right] \quad (4)$$

or

$$SN_m = SN + E_R$$

A typical value of  $E_R$  for the current data lies in the range  $1.0 < E_R < 1.5$  corresponding to  $e_1, e_2$  in the range  $0.005 < e < 0.05$ . Equation (4) indicates that the high percentage deviation of the data at small SN (generally  $SN < 10$ ) is to be expected (Fig. 10).

The measured value of the ratio  $R_S/R_W$  may be inaccurate due to two causes. The first is that the measurement of the reflectance of the clean filter paper may be incorrect ( $e_2$ ). It was found that the reflectance of the clean, Whatman No. 4, filter paper used in this study varied 2 percent about its mean value. But, this variation has only a small effect on the value of SN as is seen from Eq. (4). A second possible cause of inaccuracy in the  $R_S/R_W$  ratio is deposition of only slight amounts of particulate matter on the filter which occurs when samples are taken at the edges of the plume, at low power levels, and from "cleaner" sources. When too little material is deposited, measurement errors of the reflectometer become quite significant since the reflectance change is small and difficult to measure. The sample mass specification in Ref. 4 prevents overloading the filter but does not allow large enough samples to be taken for reasonable accuracy if the particulate concentration is for any reason low.

#### 4.5 OPERATIONAL EXPERIENCE

The use of a reflectometer to determine the relative particle quantity deposited on the filter paper, contributed to experimental error. Significant variations in the measurement of the reflectivity of a sample could be easily caused by varying the pressure of the operator's hand on the instrument. This difficulty was avoided however. A transmission measurement of the entire deposited sample would be preferable to a spot (in this case 1/8-in.-diam) reflectance measurement.

Smoke number (SN) and relative smoke number (SNR) are defined by ARP 1179 only at the exit nozzle plane. However, from the experience gained in this study, the definitions of SN and SNR are useful for determining relative particle concentrations in the far field exhaust plume of a turbine engine. The measurement of SN and SNR is dependent on keeping the mass of particulates deposited on the filter (rather than total air mass flow through the filter) within a certain range. It might be possible to extend the useful range of the present method by specifying that the total air mass flow through the filter should be experimentally adjusted so that the amount of particles deposited on the filter allows the determination of reasonably accurate SN values. The SNR measurements would then need to be related to the definition in ARP 1179, perhaps by use of expressions developed in Appendix IV. This would allow the method specified in ARP 1179 to be accurately extended to measurement of SNR values of present turbojet engines in the far flow field, as well as measurement of more advanced and hopefully much cleaner, turbojet engines.

An additional justification for definition of SN and SNR downstream of the nozzle exit is that significant changes may occur in the chemical composition of the exhaust gases between the nozzle exit plane and several nozzle diameters downstream, i.e., at the engine exit the flow may not be in chemical equilibrium (Ref. 3). Since total resultant pollution production is of primary interest in definitive and regulatory measurements, measurement of both gaseous and particulate pollutants for these purposes will most probably need to be made several feet downstream where there is an equilibrium concentration of all phases and species.

A tentative expression relating SN, W/A, and  $n_{p_{\infty}}$  has been developed from elementary considerations in Appendix IV. The reduction of SN data in terms of  $n_{p_{\infty}}$  shows promise of reducing some of the deviation from the mean which is observed in the SNR data.

It was found (see Section IV) that, for this measurement system and this engine, it was not necessary to wait a full 5 min after engine stabilization before beginning the sampling procedure as is required in ARP 1179, Section 3.6 (Ref. 4). This allowed a higher data collection rate and extension of the measurements to afterburner power levels.

## SECTION V SUMMARY OF RESULTS

The performance of a system fabricated in general accordance with the Society of Automotive Engineers Aerospace Recommended Practice No. 1179 for the measurement of smoke emissions from turbine engines was determined. The smoke emissions characteristics and the distribution of smoke in the exhaust plume of a J85-GE-5 engine operating at ground level were determined. The significant results are as follows:

### 5.1 SMOKE EMISSIONS MEASUREMENT SYSTEM

1. The system used to measure smoke emissions was shown to provide a method of quantifying the relative smoke emissions from a turbojet engine even without visible smoke in the plume.

2. The technique specified in ARP 1179 was determined to introduce uncertainties of approximately  $\pm 1.5$  units in the relative smoke numbers calculated, as a result of reflectance measurement errors.
3. Quantification of smoke emissions at positions other than the nozzle exit (as specified in ARP 1179) was demonstrated to be feasible. However, for emissions yielding relative smoke numbers less than approximately 5, the specified procedure did not provide adequate particulate deposition for accurate smoke emission determination.
4. The specified requirement of maintaining the engine on condition for 5 min while sample flow was drawn through the transfer line was shown to be unnecessary. A time of 1 min was shown to be adequate.
5. The ARP 1179 specifies an uncooled probe. Smoke emissions at afterburning power near the nozzle exit require the use of a cooled probe because of the high ( $>3000^{\circ}\text{R}$ ) exhaust gas temperatures.

## 5.2 ENGINE EMISSION CHARACTERISTICS

1. The quantity of smoke emitted by the J85-GE-5 engine at static conditions increased with power from idle to maximum dry power (military) and decreased with increasing afterburner power; at maximum afterburning, it was nearly at the level emitted at idle.
2. Radial profiles of smoke intensity at a fixed power as a function of distance indicate that only the expected turbulent mixing (external to the inviscid core) occurred in the plume. Within the inviscid core, a rapid decrease of smoke intensity was observed at the higher power levels.
3. Wind shift of the plume (maximum crosswind component of 7 mph) was not observed within 16 ft of the nozzle exit except for idle power.
4. Effects of changing ambient temperature or humidity (29 to  $80^{\circ}\text{F}$ , 20 to 50 percent relative humidity) on the smoke data were not discernible.

## REFERENCES

1. Durrant, T. "The Reduction of Smoke from Gas Turbine Engines." Aircraft Engineering, Vol. 41, No. 7, July 1969, pp. 28-31.
2. Taylor, W.G., et. al. "Reducing Smoke from Gas Turbines." Mechanical Engineering, Vol. 90, No. 7, July 1968, pp. 29-35.
3. Lazalier, G.R. and Gearhart, J.W. "Measurement of Pollutant Emissions from an Afterburning Turbine Engine at Ground Level. Part II. Gaseous Emissions" AEDC-TR-72-70, 1972.

4. SAE Committee E-31. "Aircraft Gas Turbine Engine Exhaust Smoke Measurement." Aerospace Recommended Practice 1179, May 1970.
5. Champange, D.L. "Standard Measurement of Aircraft Gas Turbine Engine Exhaust Smoke." ASME Paper 71-GT-88. March 1971.
6. Salee, G.P. "Standard Smoke Measurement Method." SAE Paper 700250. April 1970.
7. General Electric Company. "Model Specification E1024-B, Engine Aircraft, Turbojet J85-GE-5." June 30, 1960.
8. "US Gas Turbine Engines." Aviation Week and Space Technology, 94, 80, 1971.
9. Brunauer, S. The Adsorption of Gases and Vapors, Volume I. Princeton University Press, London, 1945.
10. Holman, J.P. Heat Transfer. McGraw-Hill Book Company, 1963.
11. Faehl, K.C., Turner, E.E., and Kistler, S.M. "Afterburner Altitude Characteristics and General Performance of the J85-GE-5 Turbojet Engine, Appendix B, Tabulated Data." AEDC-TN-61-57 (AD257724), June 1961.

**APPENDIXES**

- I. ILLUSTRATIONS**
- II. TABLES**
- III. METHOD OF DATA REDUCTION**
- IV. A TECHNIQUE FOR THE REDUCTION  
OF SMOKE NUMBER DATA**

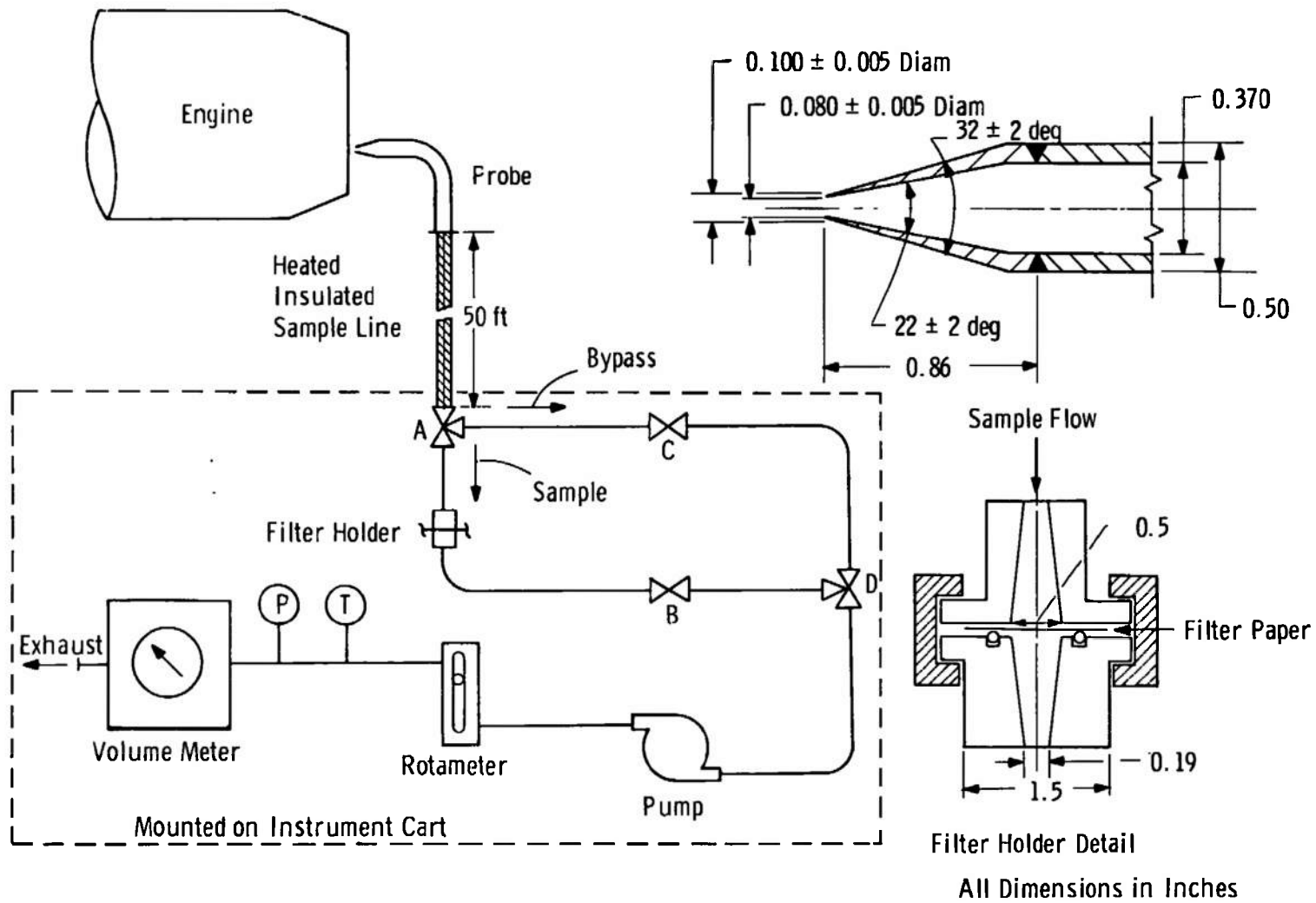
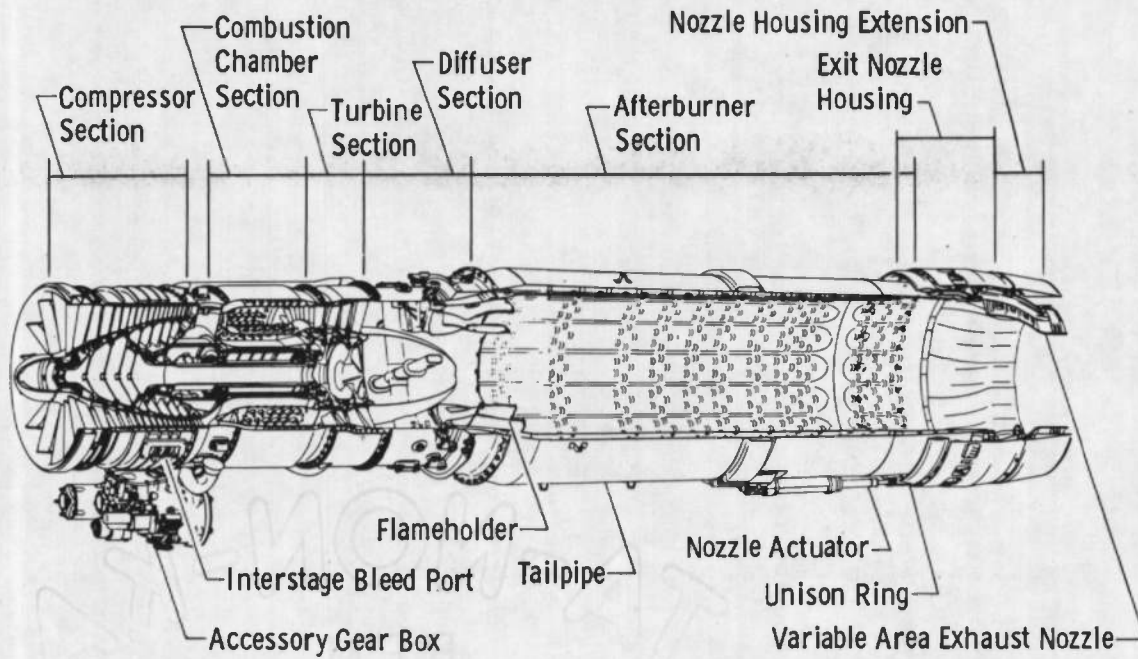
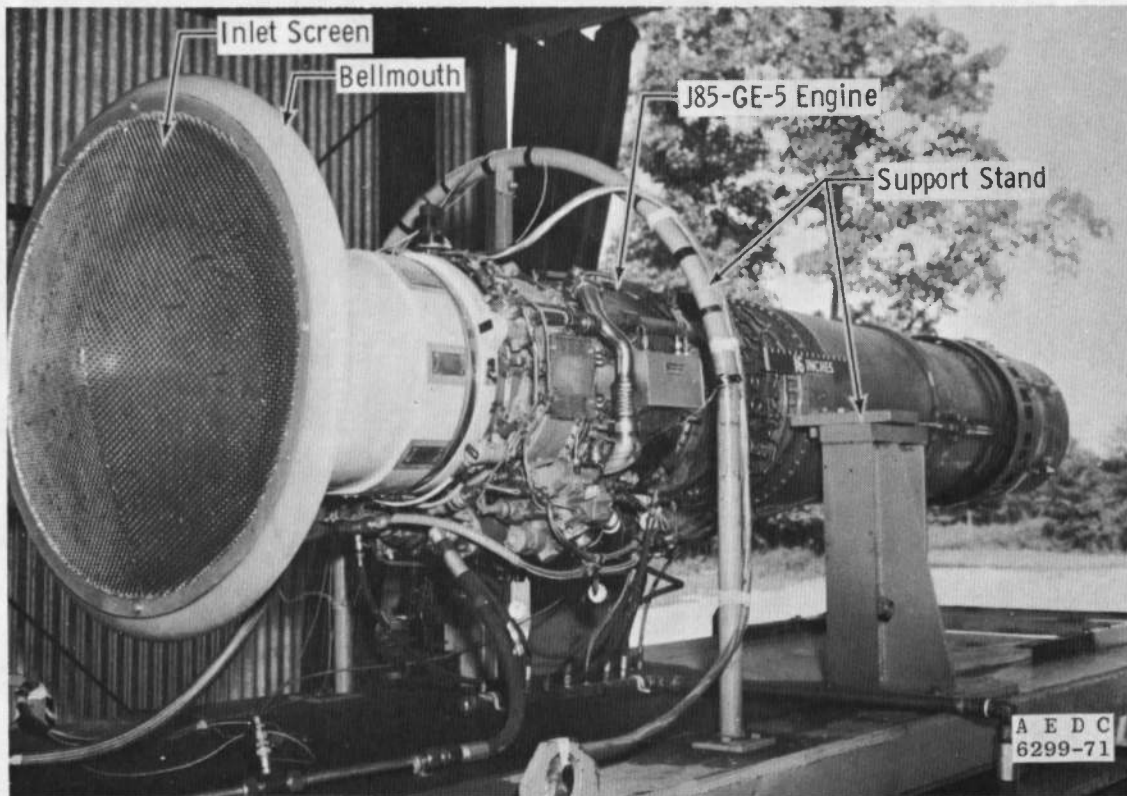


Fig. 1 Schematic of Smoke Sampling System



a. Cutaway Section



b. Photograph  
Fig. 2 J85-GE-5 Turbojet Engine

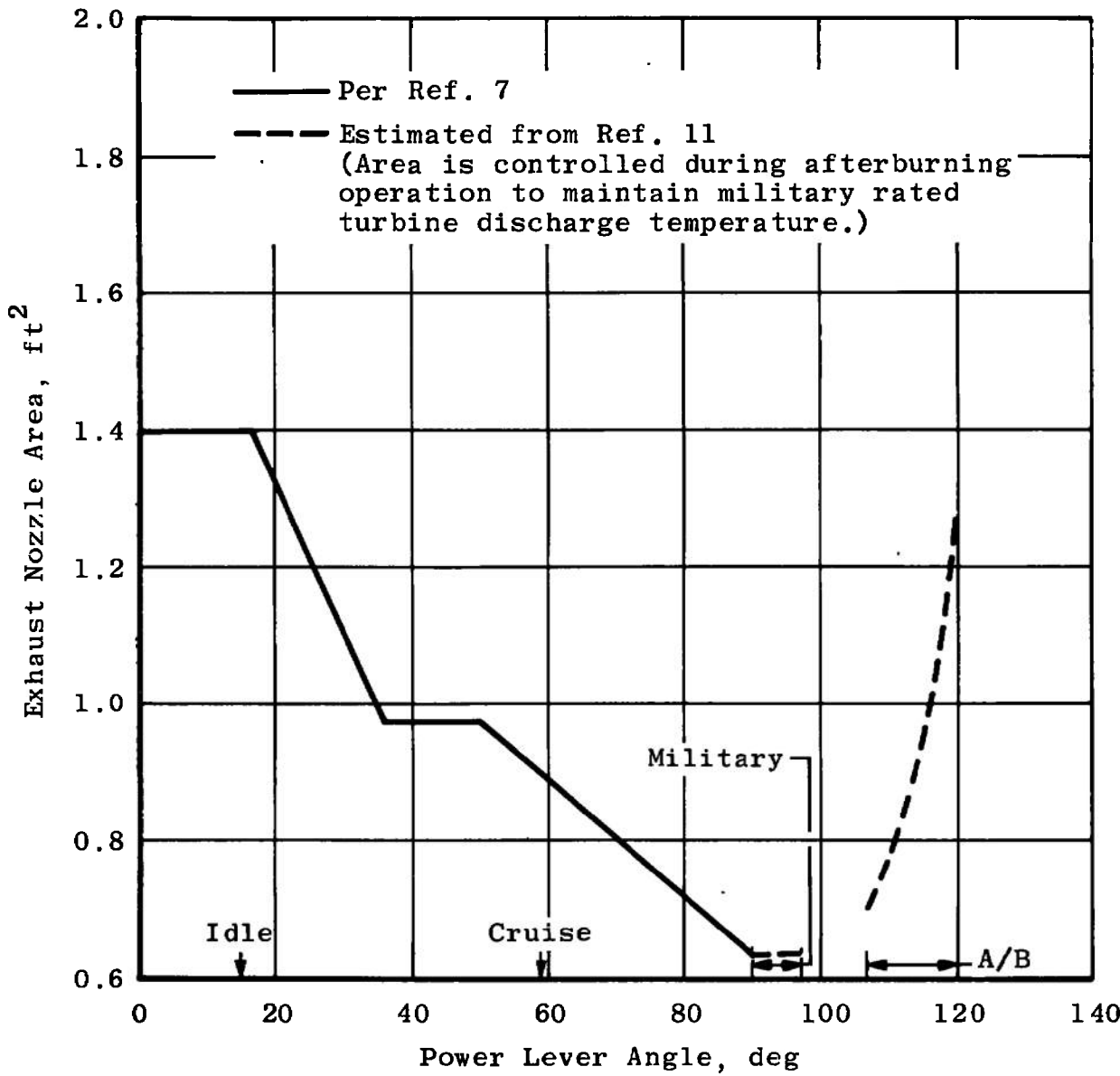
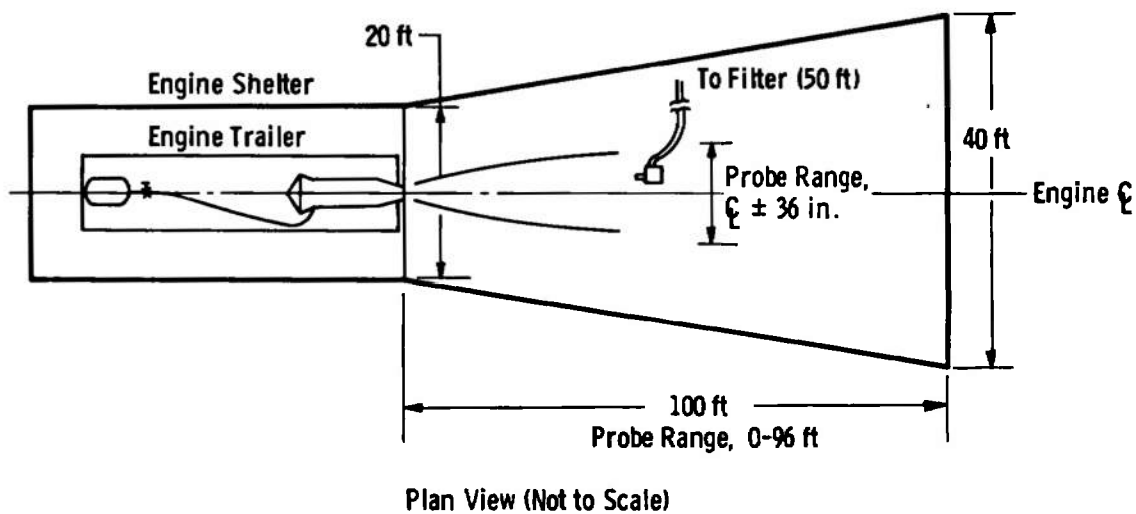
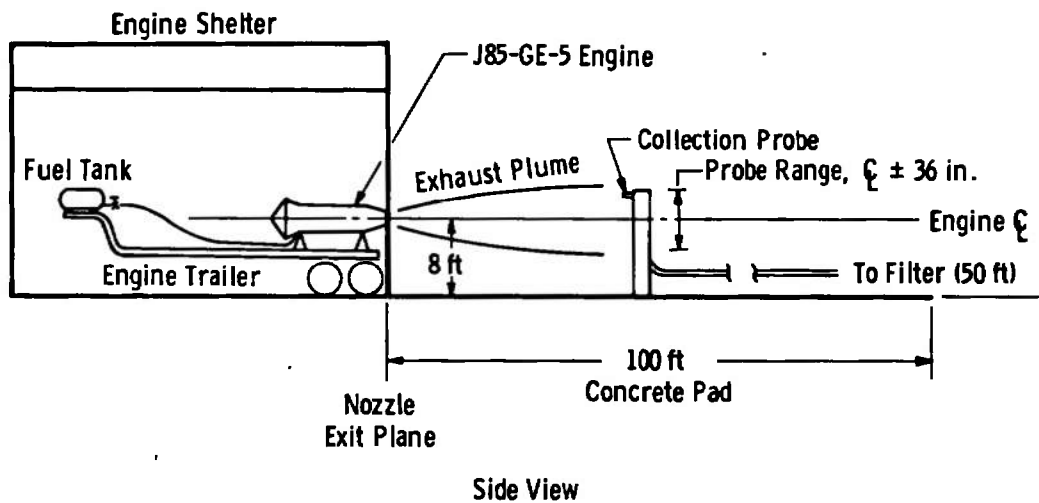
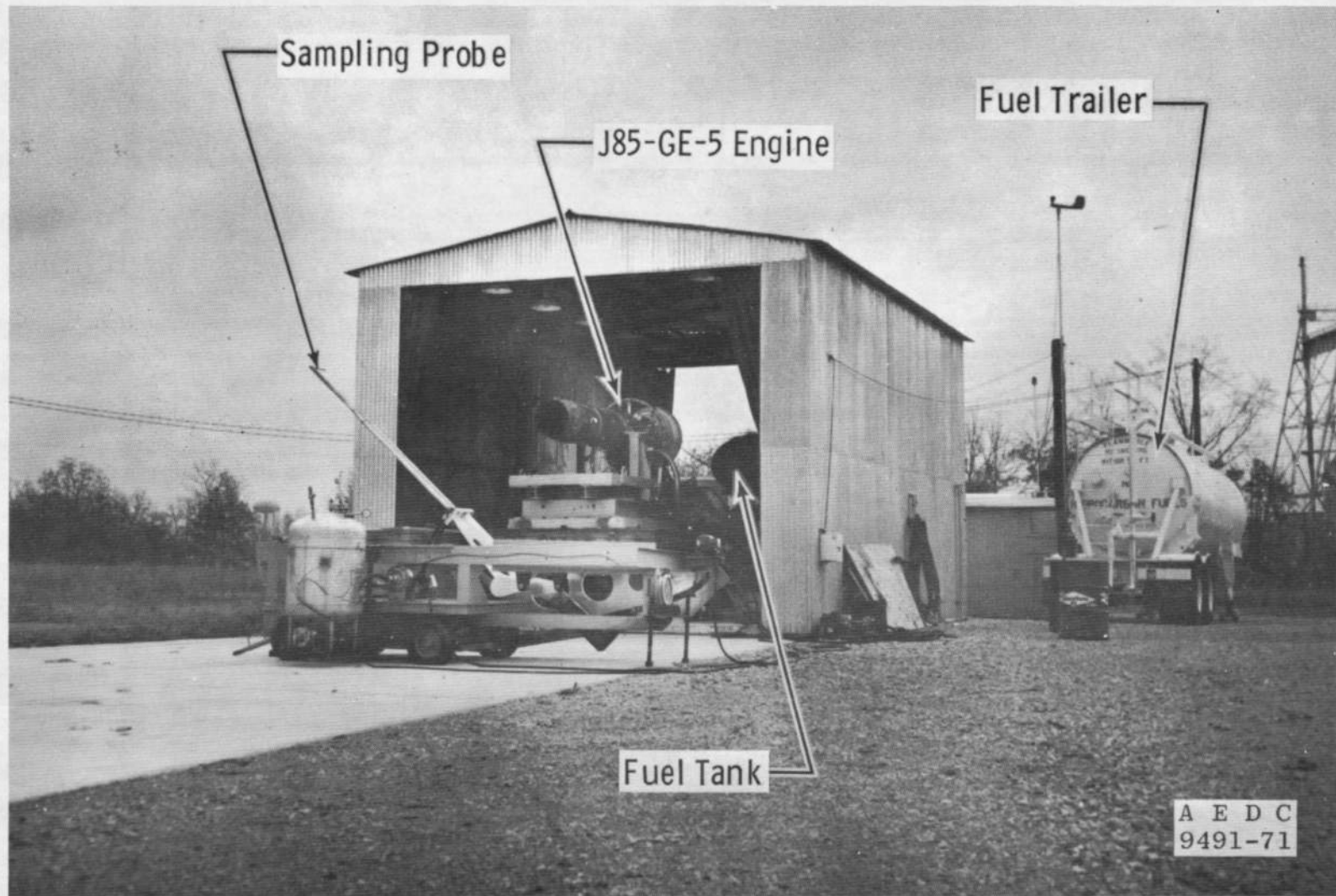


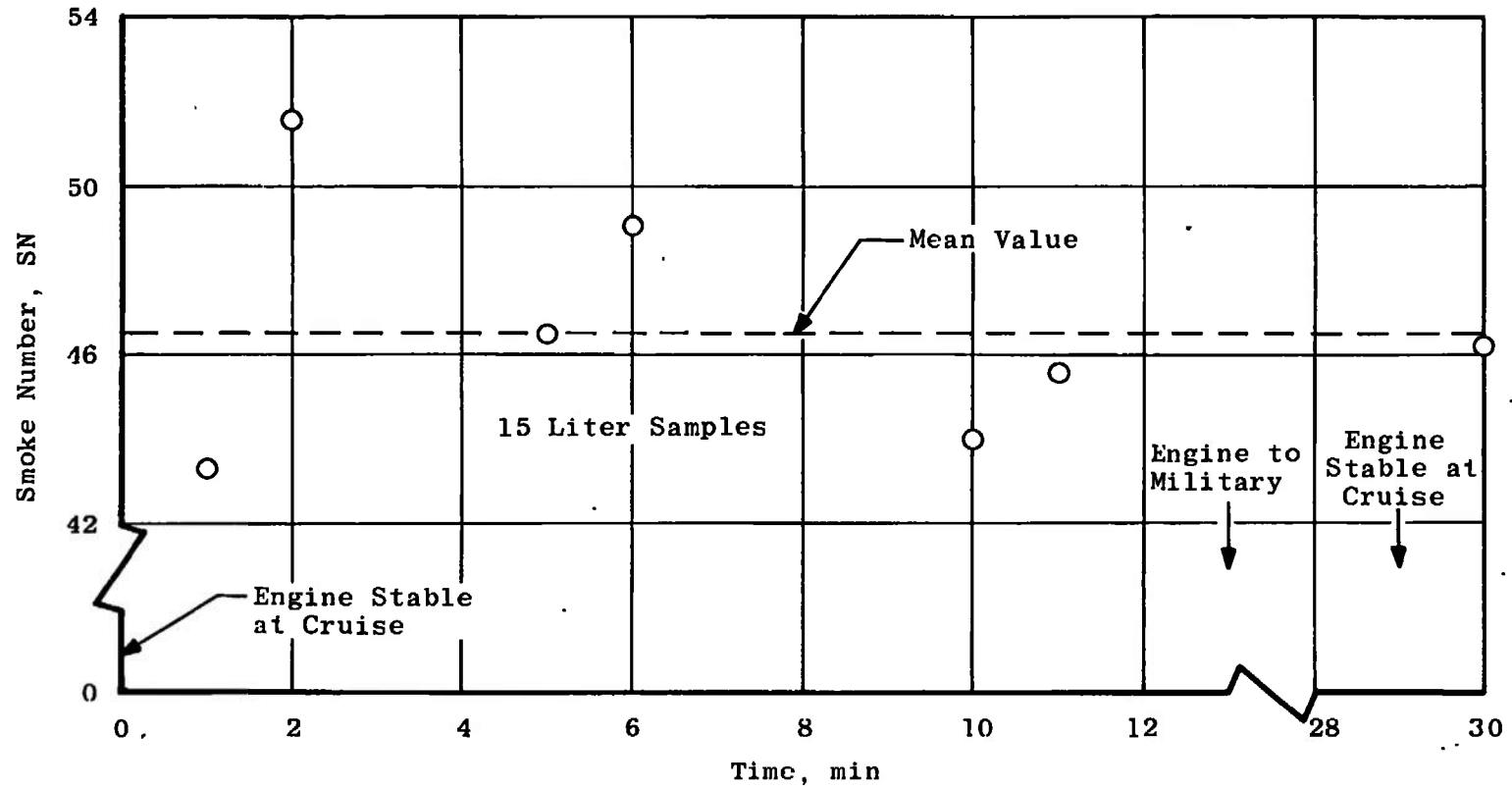
Fig. 3 Exhaust Nozzle Area versus Power Lever Angle



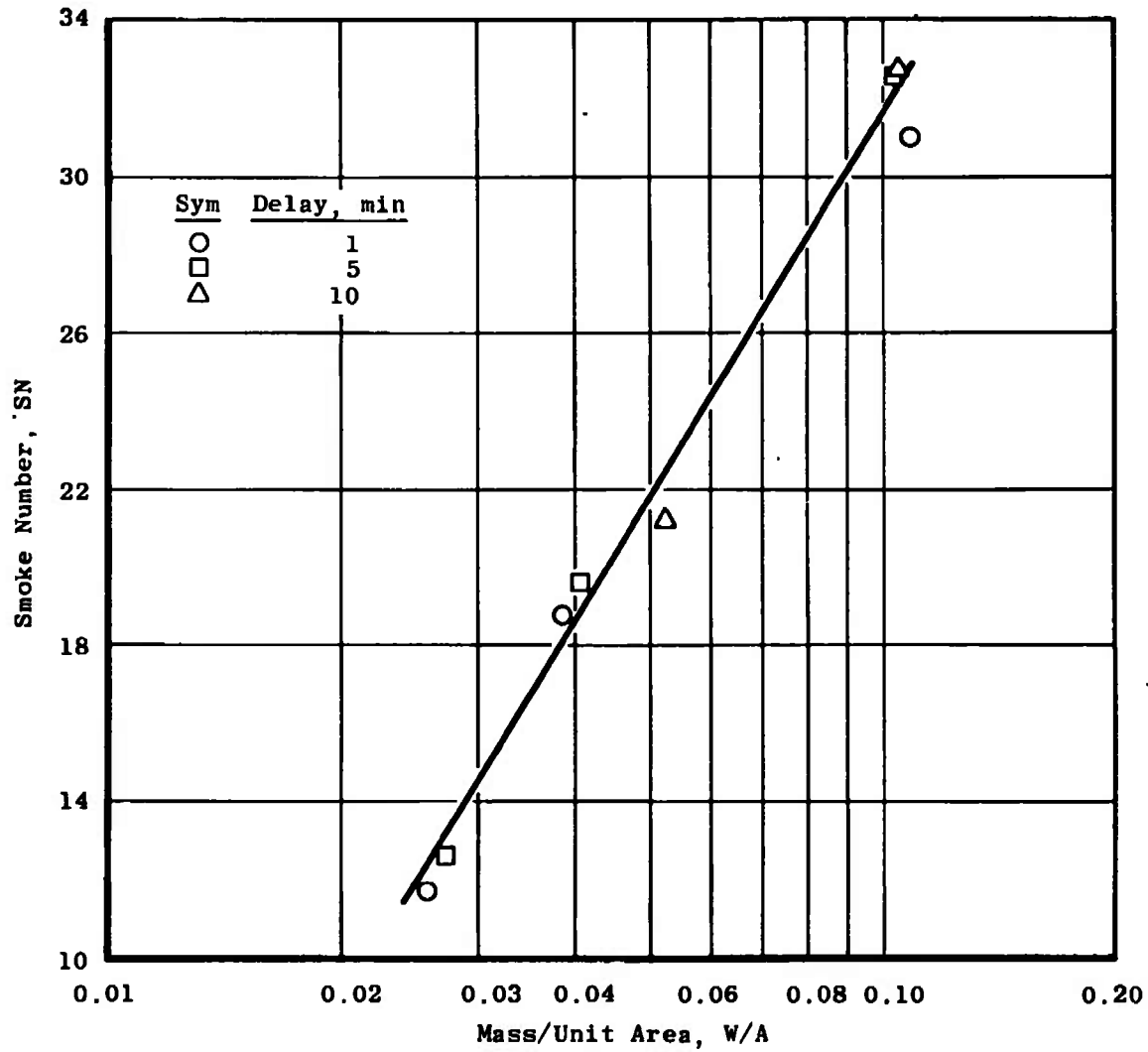
a. Schematic  
 Fig. 4 Ground Level Test Stand



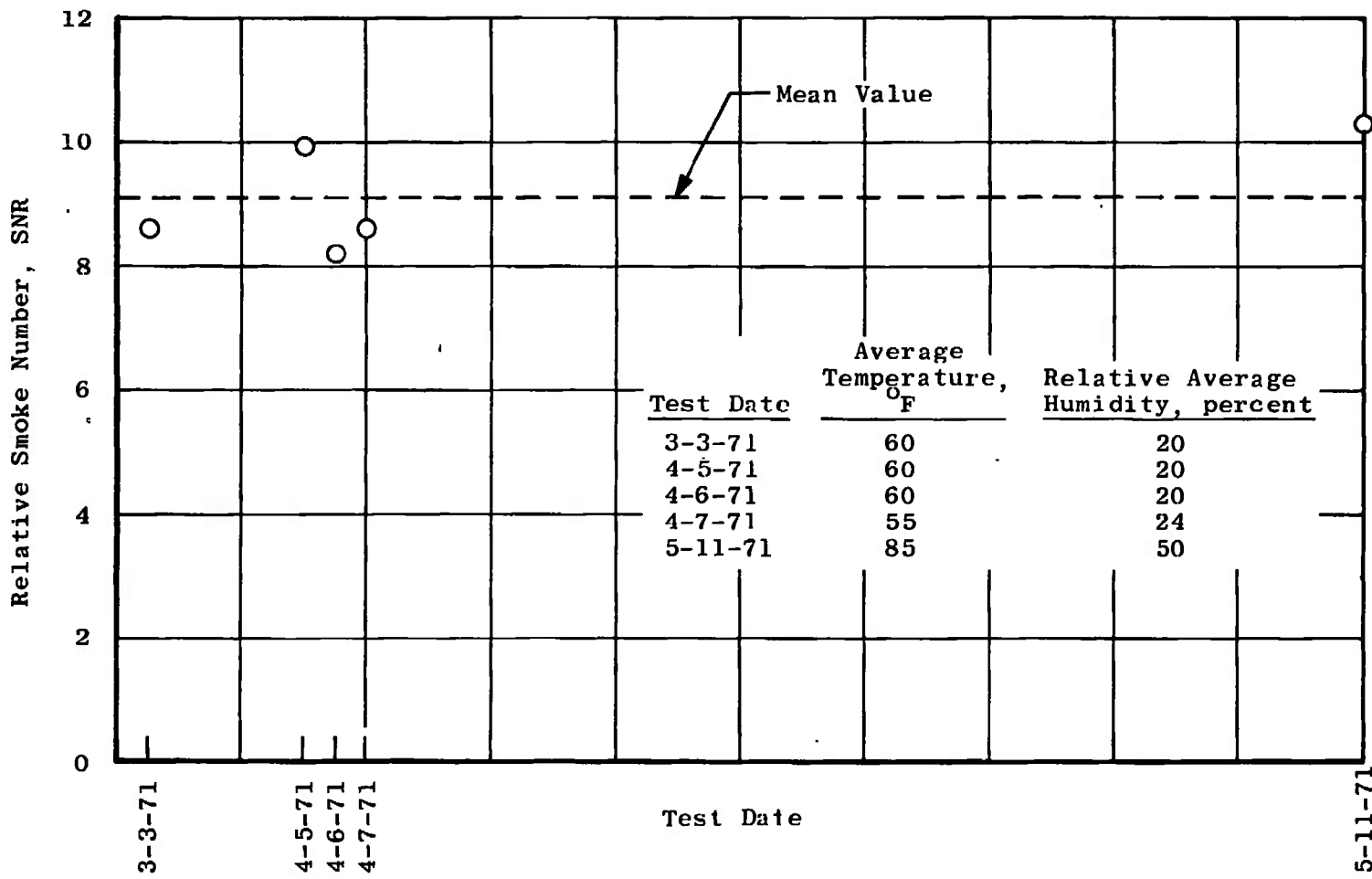
b. Photograph  
Fig. 4 Concluded



a. SN, 1 ft Aft, Cruise  
Fig. 5 Variation on Centerline



b. SN, 2 ft Aft, Military  
Fig. 5 Continued



c. SNR, at the Nozzle Exit, Cruise  
Fig. 5 Concluded

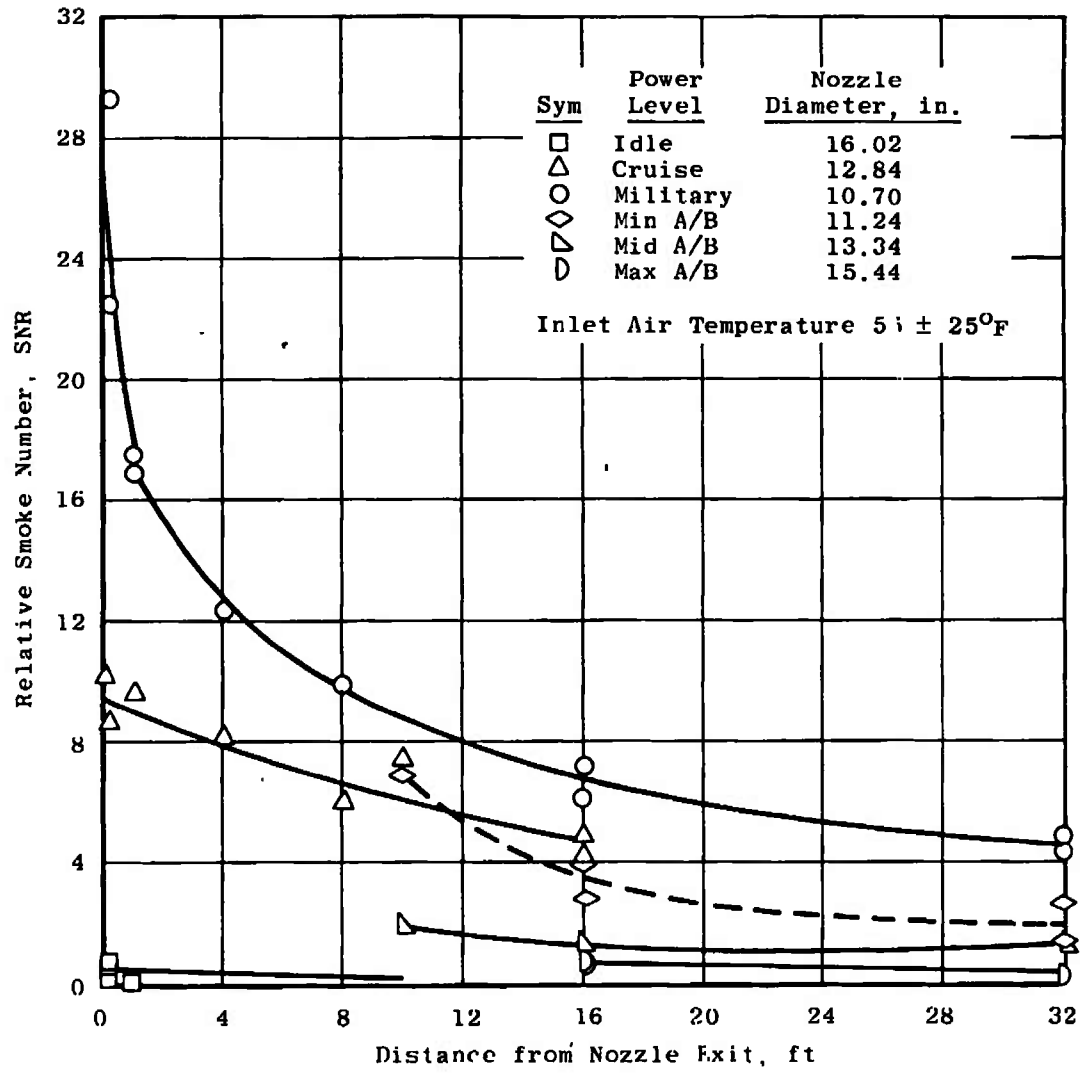
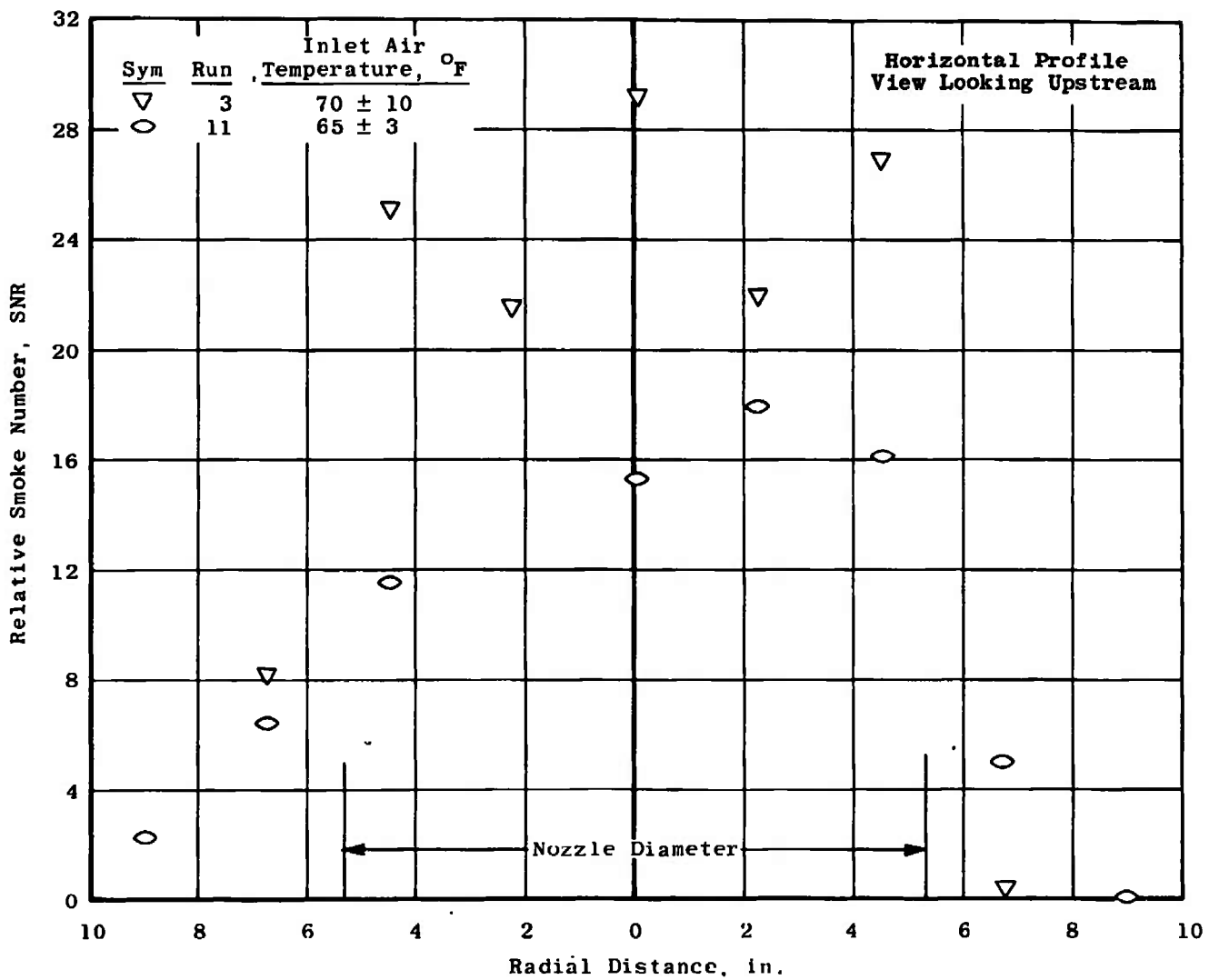
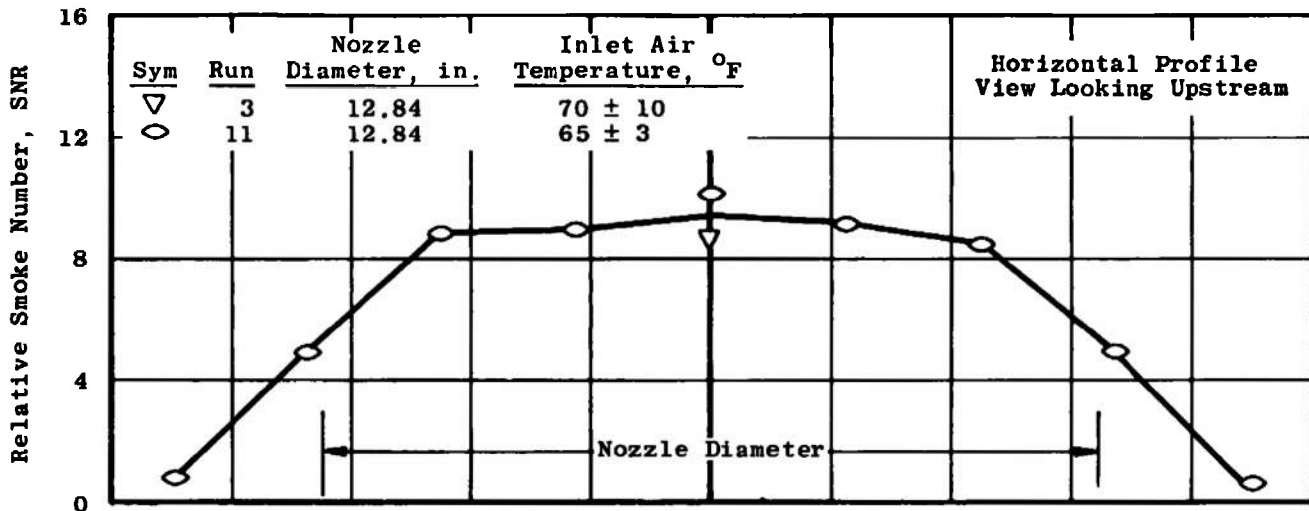


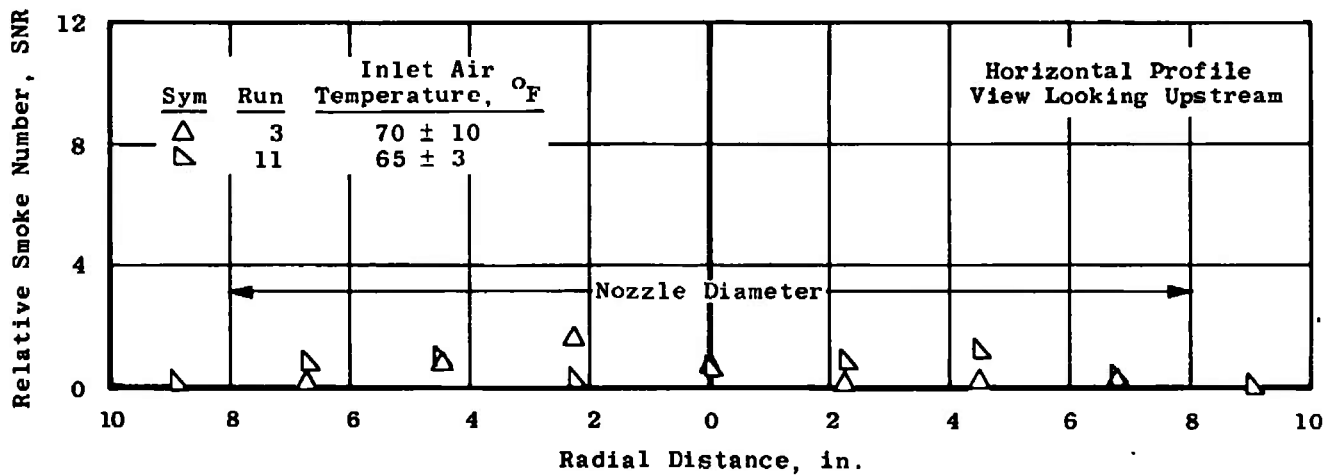
Fig. 6 Centerline Smoke Values as a Function of Distance



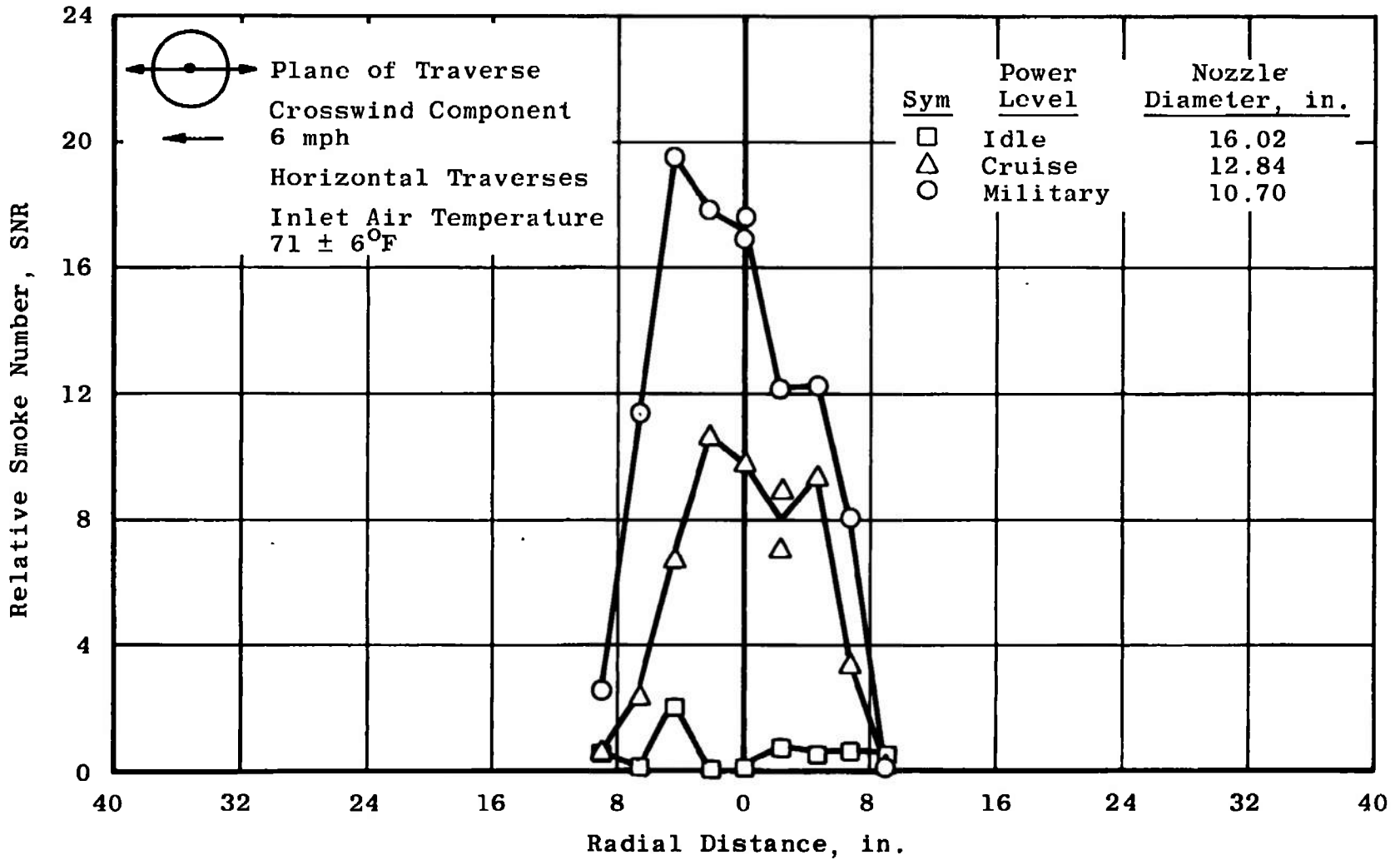
a. Military Power  
 Fig. 7 SNR Profile at Nozzle Exit



b. Cruise Power

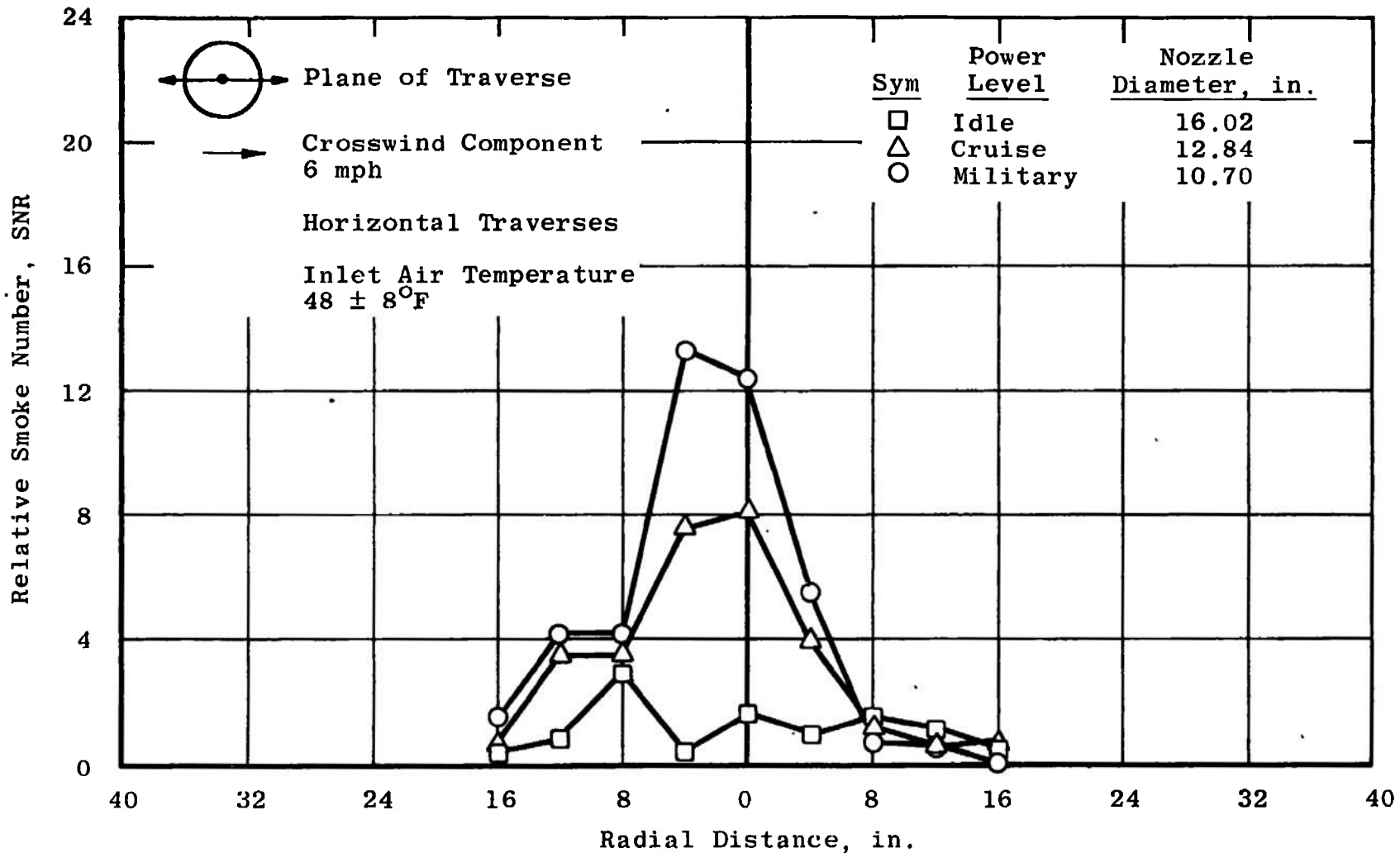


c. Idle Power  
Fig. 7 Concluded

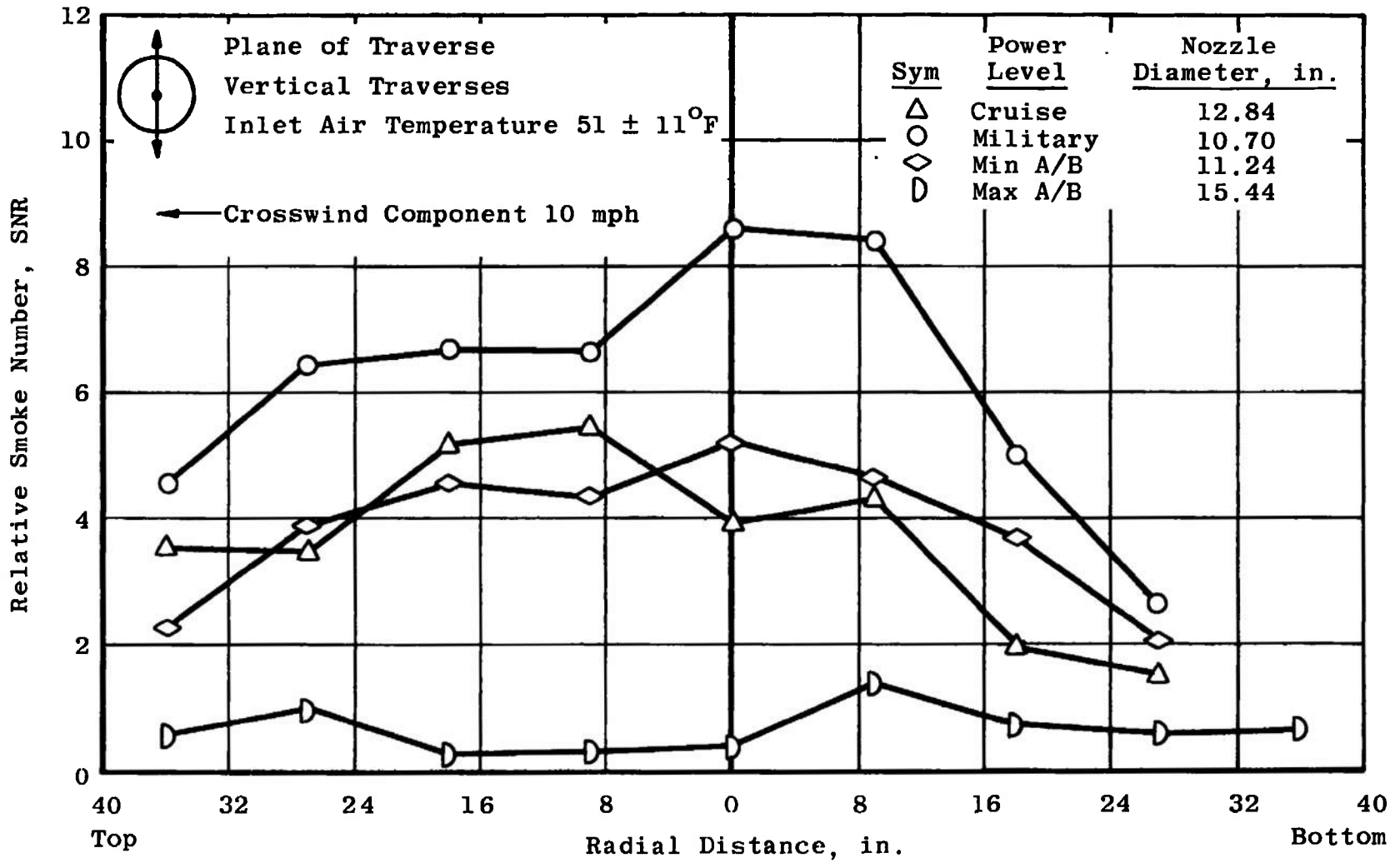


24

a. 1 ft Aft of Nozzle Exit  
 Fig. 8 Radial Profiles on SNR (View Looking Upstream)



b. 4 ft Aft of Nozzle Exit  
Fig. 8 Continued



c. 16 ft Aft of Nozzle Exit  
Fig. 8 Concluded

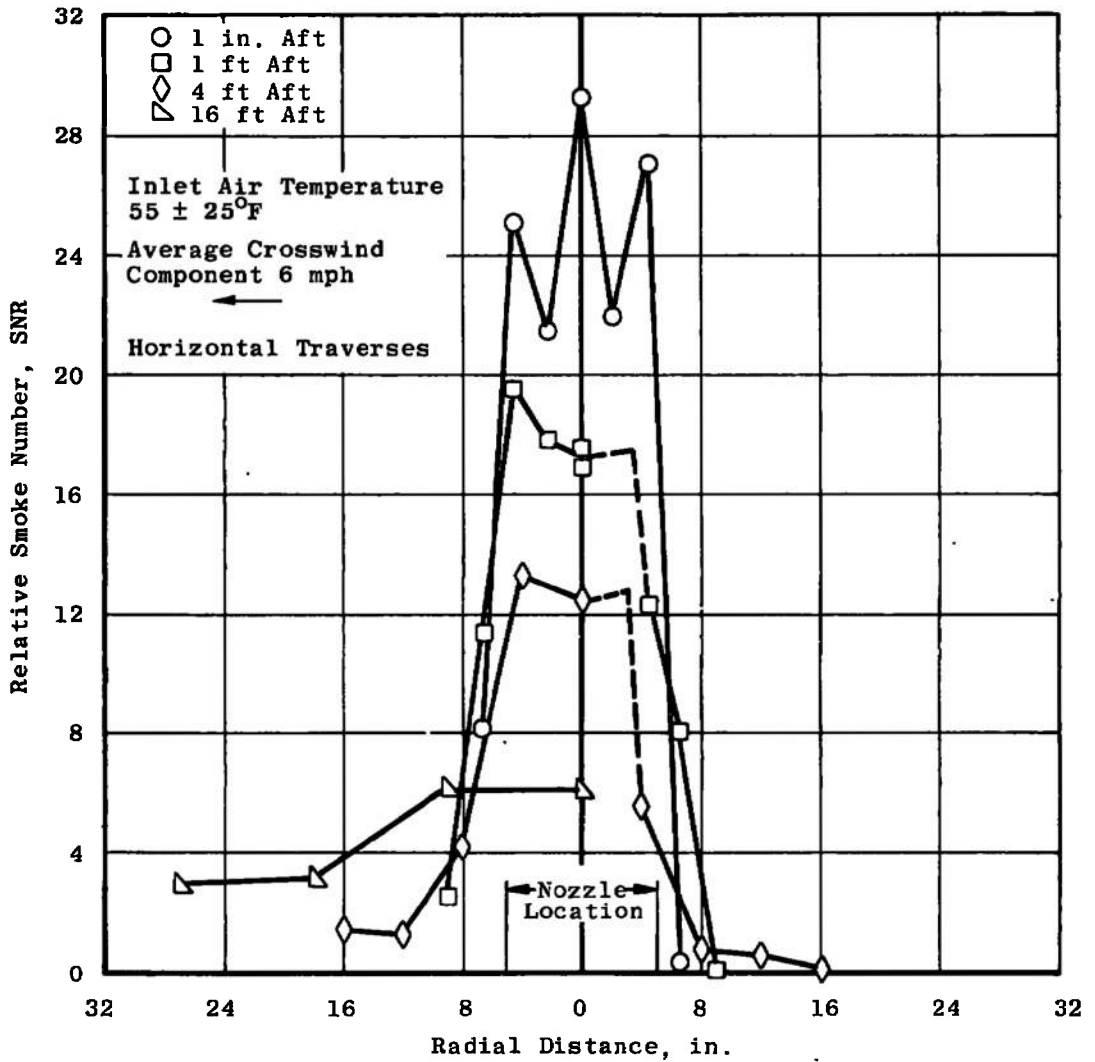
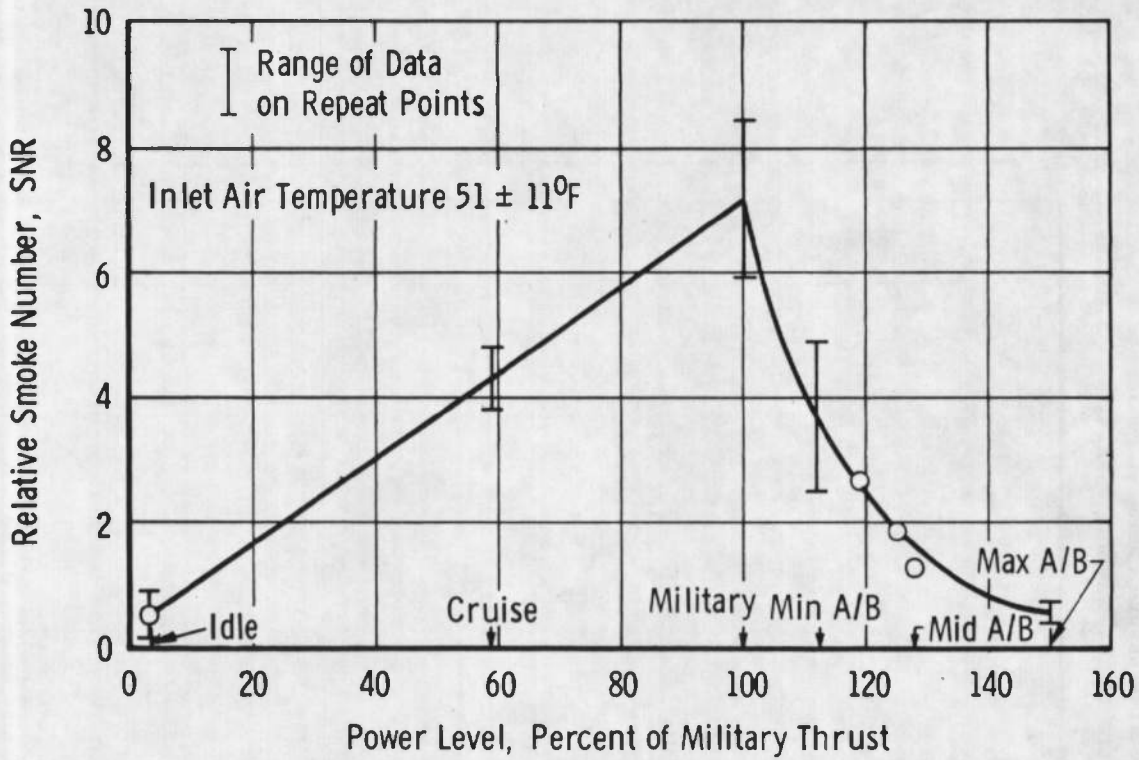
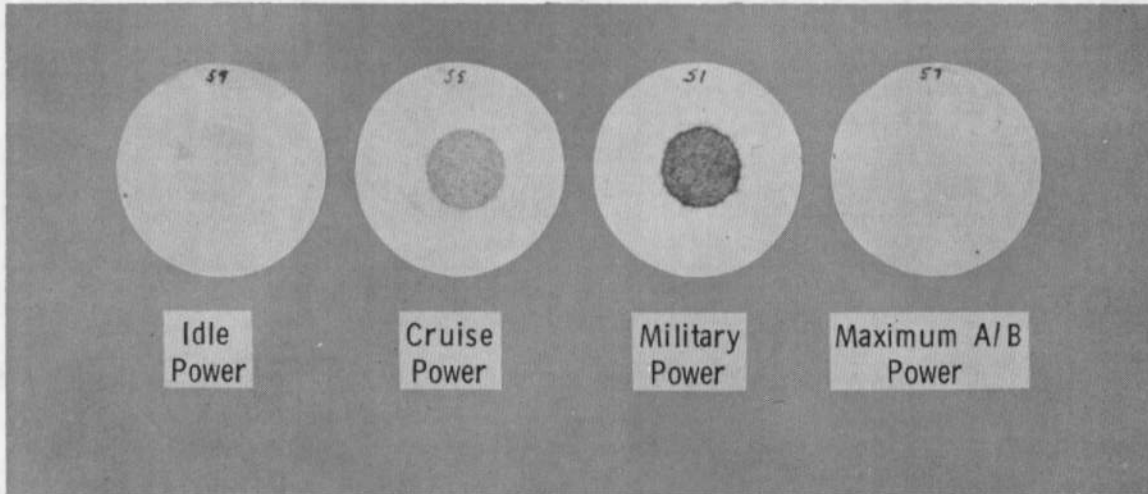


Fig. 9 Effects of Distance on SNR Profiles at Military Power (View Looking Upstream)



a. On SNR Values



b. On Filters—Photograph

Fig. 10 Effect of Power Level at 16 ft Aft of the Nozzle Exit on the Engine Centerline

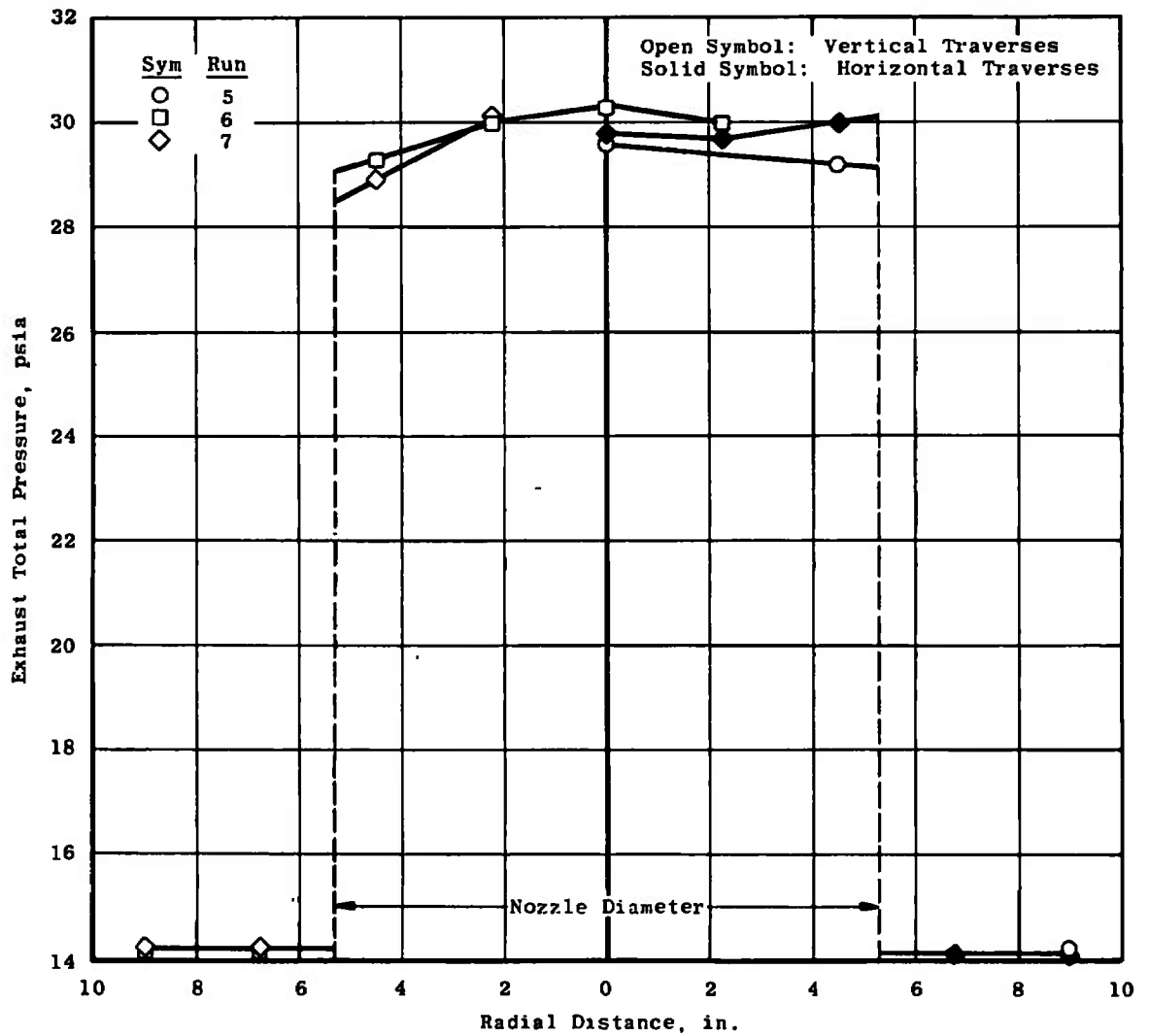


Fig. 11 Profiles of Exhaust Total Pressure at the Nozzle Exit, Military Power

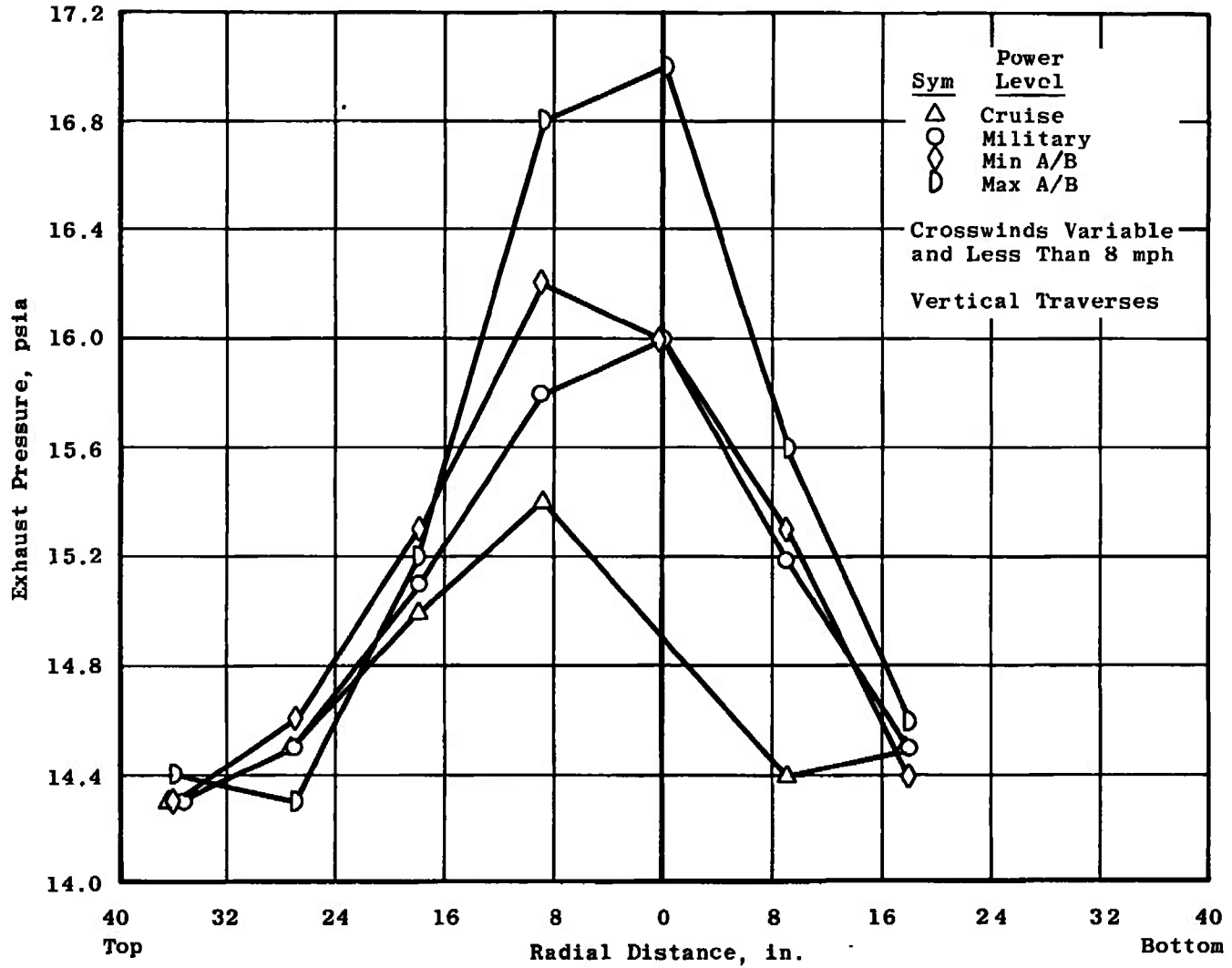


Fig. 12 Profiles of Exhaust Total Pressure at 16 ft Aft of the Nozzle Exit at Various Power Levels

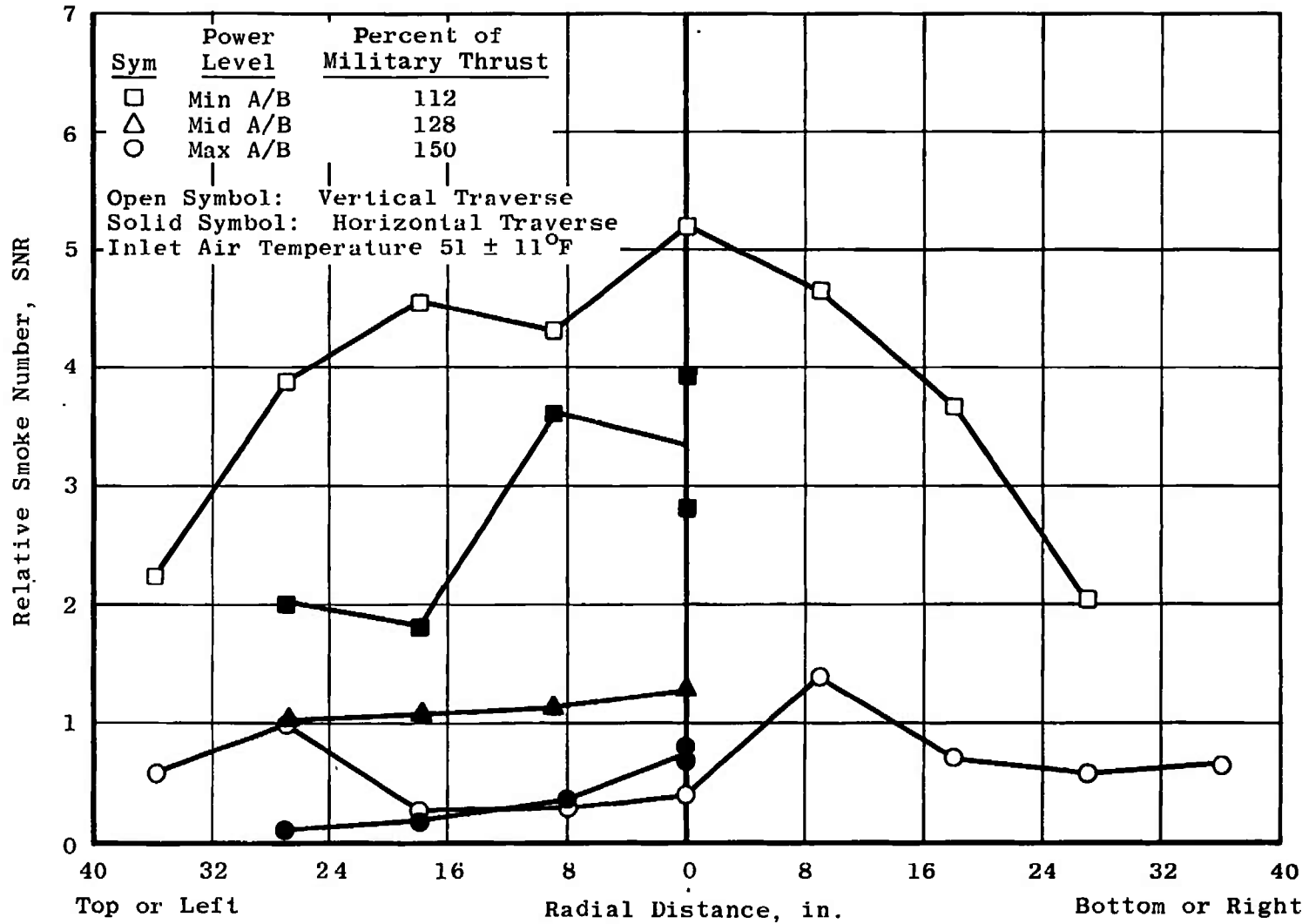


Fig. 13 SNR Profiles at Afterburner Power, 16 ft Aft of the Nozzle Exit

TABLE I  
ENGINE OPERATION PARAMETERS AT  $P_{inlet} = 14.2$  psia,  $T_{inlet} = 59^{\circ}$ F

Nominal Power Level	Engine Airflow, lbm/sec	$\frac{\text{Thrust}}{\text{Thrust at Military}} \times 100$	Engine Speed, N, percent Rated	Fuel Flow, lbm/hr		Exhaust Gas Temperature, EGT, $^{\circ}$ R	Calculated Turbine Inlet Temperature, $^{\circ}$ R (Ref. 3)	Time Limit of Power
				Engine	A/B			
Idle	12.5	3.0 percent	50.0	650	---	1460	---	Continuous
Cruise <sup>1</sup>	37.6	59.0 percent	95.0	1800	---	1610	1785	Continuous <sup>1</sup>
Military	42.5	100.0 percent <sup>4</sup>	100.0	2650	---	1710	2150	30 min
Minimum A/B	42.5	112.0 percent	~100.0	2650	1000	---	2150	--- <sup>2</sup>
Middle A/B	42.5	128.0 percent	~100.0	2650	2950	---	2145	--- <sup>2</sup>
Maximum A/B	42.5	150.0 percent	~100.0	2650	4050	~3300 <sup>3</sup>	2140	5 min

<sup>1</sup>Maximum Power for Continuous Operation

<sup>2</sup>Not Specified

<sup>3</sup>Nozzle Discharge Temperature

<sup>4</sup>Thrust at Military Power with Inlet Temperature of 519 $^{\circ}$ R is Approximately 2450 lbf

**TABLE II  
CHEMICAL COMPOSITION OF JP-4 FUEL**

Constituent	Maximum Allowable
Sulfur	0.4 percent weight
Mercaptan Sulfur	0.001 percent weight
Aromatics	25.0 percent volume
Olefin	5.0 percent volume
Particulate Matter	8.0 mg/gal
Fuel System Icing Inhibitor	0.15 percent volume <sup>2</sup>
Anti-Oxidants <sup>3</sup>	9.1 g/100 gal
N, N' - Diisopropyl-para-phenylenediamine	
N, N' - Disecodary Butyl-para-phenylenediamine	
2, 6 Ditertiary Butyl-4-methylphenol	
2, 4 Dimethyl-6-Tertiary butylphenol	
2, 6 Ditertiary Butylphenol	
75-percent Minimum 2, 6 - Ditertiary Butylphenol and 25-percent Maximum Tertiary and Tritertiary Butylphenols	

<sup>1</sup>The fuel shall consist completely of hydrocarbon compounds except as specified in MIL-T-5624G.

<sup>2</sup>Minimum of 0.10 percent volume.

<sup>3</sup>Listed items may be blended separately or in combination not in excess of specified limit.

### APPENDIX III METHOD OF DATA REDUCTION

The data necessary for calculation of relative smoke number (SNR) included engine conditions; sample pressure, temperature, and volume; and the measurement of the reflectivity of the filter paper before ( $R_W$ ) and after ( $R_S$ ) the sampling process.

Smoke number (SN) is defined by Ref. 4 to be

$$SN = 100 \left[ 1 - \frac{R_S}{R_W} \right]$$

Four samples (each of different volume and in the range specified by Ref. 4) were taken at each position and power setting of interest. The SN's from these samples were plotted on a semilogarithmic scale against  $W/A$  (Fig. III-1), where  $W/A$  was defined to be the mass of air, in pounds, drawn through the filter while taking the sample divided by the area of the filter in the stream ( $0.196 \text{ in.}^2$ ),  $W$  was defined by Ref. 4 to be  $W(\text{lbm}) = 1.326 pV/T$ , where  $p$  is in inches of mercury absolute,  $V$  is in  $\text{ft}^3$ , and  $T$  is in  $^\circ\text{R}$ . The relative smoke number (SNR) was found, in accordance with Ref. 4, by fitting a straight line through the SN versus  $\log W/A$  data by the method of least squares and determining the value of this straight line function at  $W/A = 0.0230 \text{ lbm (sample gas)/in.}^2$  (filter) as shown in Fig. III-1.

The resulting SNR values were then plotted against percent of military thrust of the engine. Figure III-2 shows a typical plot of these data.

All of the above calculations and plots were made by computer. Additional tabulations provided by the computer included the input values for each point ( $R_S$ ,  $R_W$ ,  $A_t$ , volume of the sample, pressure of the sample, sample power setting), and the temperature and calculated values of  $W$ ,  $\log W/A$ , SN, and the SNR value for each test point, as well as the maximum deviation of the points from the least-squares line fit.

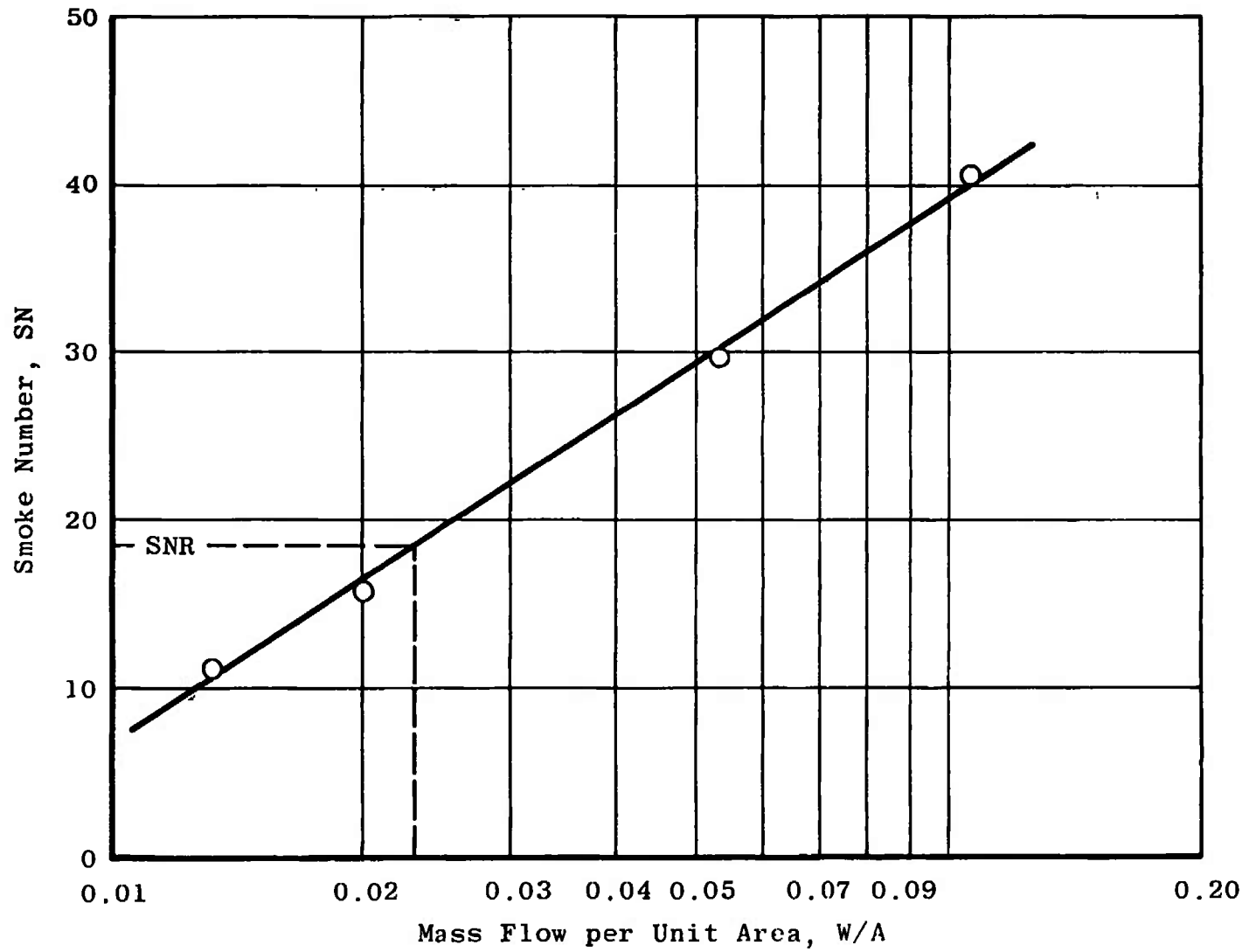


Fig. III-1 Typical SN versus W/A Plot

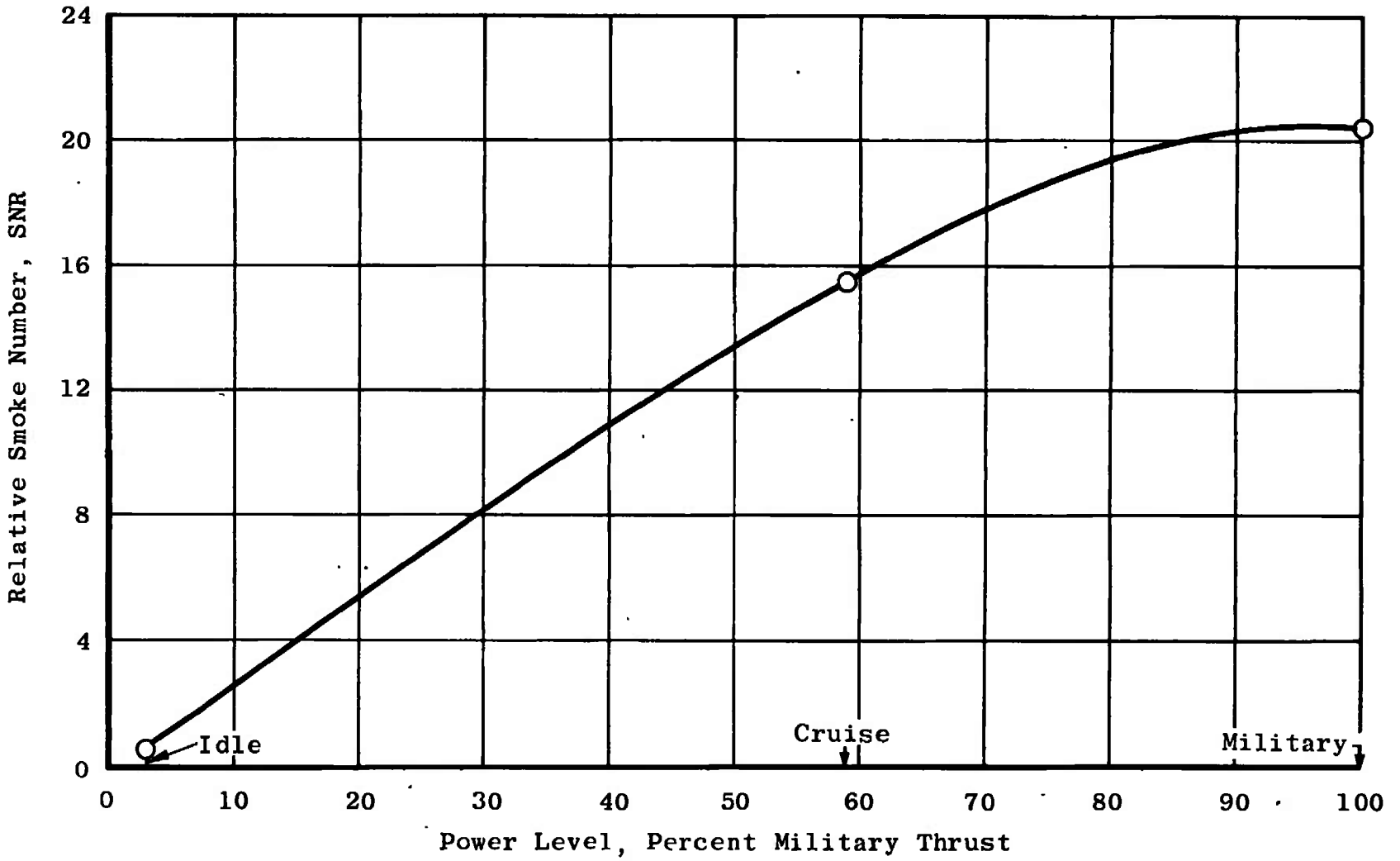


Fig. III-2 Typical Plot of SNR versus Power Level

## APPENDIX IV A TECHNIQUE FOR THE REDUCTION OF SMOKE NUMBER DATA

The smoke number has long been established as an acceptable technique for quantizing particulate suspensions in air, i.e., smoke (Ref. 5). The method is not only easy to use but it is also inexpensive to operate and maintain. The only objectionable feature of the technique is that the relationship between SNR and the more descriptive parameters of the particulate concentrations, such as number density ( $n_{p\infty}$ ), have remained unestablished. A tentative expression for this relationship is derived in this section and a favorable comparison with the data is obtained<sup>1</sup>.

The principle on which the SN measurement is based is that there is a difference between the reflectance of the material composing the filter and the particles. Thus, the definition of SN is

$$SN = 100 (1 - R_S/R_W)$$

where  $R_W$  and  $R_S$  are, respectively, the reflectances of clean and dirty filter paper. The change in gross reflectance between the clean and dirty filter depends on the surface concentration of the particles ( $n_{ps}$ ) on the paper as well as the reflectance of the particles.

Since SN, as defined in Ref. 4, depends on  $n_{ps}$ , it is necessary to consider the interactions that an incident particle may undergo at the surface of the filter paper. These interactions may be divided into three groups (Fig. IV-1): the first group contains those which do not result in a change in the fraction of surface area occupied by the particles ( $\theta = A_p/A_t$ ); the second those which result in an increase in  $\theta$ ; and the third group those interactions which result in a decrease in  $\theta$ . The first group includes such interactions as stacking up of particles and imbedding of particles in the surface, provided no change in  $\theta$  occurs (Fig. IV-1a). The second group accounts for stacking or imbedding interactions involving a  $\theta$  increase (Fig. IV-1b). Finally, interactions such as collisions in which both particles are driven into the surface or collisions of a smaller incident particle with a larger deposited particle in which the larger is imbedded resulting in a  $\theta$  decrease are included in the third group (Fig. IV-1c). Henceforth, interactions in the last two groups will be referred to as "effective interactions."

By considering the rate at which particles are effectively deposited on the surface ( $a\mu$ ) and the rate at which particles are effectively removed ( $\nu$ ), the following expression for the net rate of change of the surface concentration ( $n_{ps}$ ) is obtained:

$$\frac{\partial}{\partial t} (n_{ps}) = a\mu - \nu \quad (IV-1)$$

---

<sup>1</sup>The authors wish to acknowledge the contributions made by Dr. K.E. Tempelmeyer who first pointed out the analogy between particle surface concentration on the filter paper and adsorption of a gas on a surface. He also suggested that the Langmuir Adsorption Theory (Ref. 9) would provide a basis for the present model.

where  $a$  is the probability that a particle striking the surface will remain on the surface and  $\mu$  is the particle strike rate (particles/cm<sup>2</sup> sec). The interactions of group 1 particles have no effect on Eq. (IV-1) and are ignored in the subsequent development. i.e.,  $a$  has no dependence on group 1 interactions.

If the effective strike ( $a\mu$ ) that changes the surface area (particles/unit area/unit time) is taken to be proportional to the uncovered area, then the approximation

$$a\mu = a_0(1 - \theta)\mu \quad (IV-2)$$

is permitted, where  $a_0$  is the value of  $a$  corresponding to a clean surface. Further, if the probability that a particle on the surface will undergo a group 3 interaction is taken to be the same whether or not the neighboring positions are occupied, then the approximation

$$\nu = \nu_1\theta \quad (IV-3)$$

can be made, where  $\nu_1$  is the removal rate from a completely covered surface. Substitution of Eqs. (IV-2) and (IV-3) into Eq. (IV-1) and rearranging yield

$$\theta = \frac{a_0\mu \cdot \frac{\partial}{\partial t}(n_{ps})}{a_0\mu + \nu_1} \quad (IV-4)$$

If Eq. (IV-4) is calculated for small values of time, where  $\theta \approx 0$ , then initially

$$\frac{\partial}{\partial t}(n_{ps}) \approx a_0\mu$$

For all later times,  $\partial/\partial t(n_{ps}) < a_0\mu$  since the rate at which  $n_{ps}$  changes is being slowed by  $\nu_1\theta$ . If it is further assumed that, for all subsequent times,  $\partial/\partial t(n_{ps})$  is a real function of time such that

$$\frac{\partial}{\partial t}(n_{ps}) \approx \text{constant} = \gamma a_0\mu$$

where  $\gamma$  is suitable constant less than one, then Eq. (IV-4) may be written as

$$\theta = \frac{a_0\mu}{\nu_1} (1 - \gamma) / \left(1 + \frac{a_0\mu}{\nu_1}\right) \quad (IV-5)$$

The strike rate ( $\mu$ ) is taken to be constant over the sampling time ( $\Delta t$ ). Then  $\mu$  is obtainable from consideration of the particle flux passing through any plane perpendicular to the flow direction, i.e.,

$$\mu = \frac{\partial}{\partial t} \left( \frac{n_p}{A} \right) = n_{p\infty} V \quad (IV-6)$$

where  $\partial/\partial t(n_p/A)$  is the number of particles passing the plane per unit time,  $n_{p\infty}$  is the free-stream number density which is assumed to be equal to the ambient value, and  $V$  is the average particle velocity. It is reasonable to expect that the particle velocity is the same as the gas velocity if the average particle size is small and the sampling line long. The continuity equation for the gas flow is

$$W = \rho A V \Delta t \quad (\text{IV-7})$$

where  $W = \Delta t m$  is the total mass flow and  $\rho$  is the gas density. Combining Eqs. (IV-6) and (IV-7) and rearranging yield

$$\mu = \frac{n_{p\infty}}{\rho} \frac{W}{A} \frac{1}{\Delta t} \quad (\text{IV-8})$$

Substitution of Eq. (IV-8) into Eq. (IV-5) gives

$$\theta = \frac{C_1 \frac{W}{A} n_{p\infty} (1 - \gamma)}{1 + C_1 \frac{W}{A} n_{p\infty}} \quad (\text{IV-9})$$

where

$$C_1 = a_o / (v_1 \rho \Delta t)$$

The reflectance of the clean filter paper may be written in terms of adsorptivity of the filter paper as

$$R_W = 1 - \epsilon_2 A_t / E_o$$

and the partially covered surface in terms of the adsorptivity of the filter paper and particles as

$$R_S = 1 - [\epsilon_1 A_p + \epsilon_2 (A_t - A_p)] / E_o$$

where  $\epsilon_1$ ,  $\epsilon_2$  are the energy adsorbed per unit area of the particles and filter paper, respectively, and  $E_o$  is the incident energy. The smoke number may now be rewritten as

$$SN = 100 \left[ \frac{A_p}{A_t} \frac{\epsilon_1 - \epsilon_2}{E_o / A_t - \epsilon_2} \right] = \beta \theta \quad (\text{IV-10})$$

where  $\beta = 100 (\epsilon_1 - \epsilon_2) / (E_o / A_T - \epsilon_2)$ . Substitution of Eq. (IV-9) into Eq. (IV-10) yields

$$SN = \frac{C_1 \frac{W}{A} n_{p\infty} (1 - \gamma)}{1 + C_2 \frac{W}{A} n_{p\infty}} \quad C_1 \equiv \beta C_2 \quad (\text{IV-11})$$

If  $n_{p\infty}$  is constant, SN becomes a function of W/A only. The slope may be evaluated in the form

$$\frac{\partial SN}{\partial \left( \ln \frac{W}{A} \right)} = \frac{K_1 (1 - \gamma)}{1 + K_2 \frac{W}{A}} = SN [1 - \theta (1 - \gamma)]$$

where  $K_1 = C_1 n_{p\infty}$  and  $K_2 = C_2 n_{p\infty}$ . For appropriately small values of  $K_2$ , the slope is seen to be a slowly varying function of W/A in the range  $W/A \leq 10^{-1}$  which is generally of interest. Thus, for these conditions,

$$\frac{\partial SN}{\partial \left( \ln \frac{W}{A} \right)} \approx \text{constant}$$

This result explains the utility of the straight line curve fit used for determining SNR (Refs. 4 and 5).

The asymptotic behavior of SN for large values of  $(W/A)n_{p\infty}$  can be obtained from Eq. (1).

$$\lim_{(W/A) n_{p\infty} \rightarrow \infty} \left[ (1 - \gamma) C_2 \beta \left( \frac{W}{A} \right) n_{p\infty} / \left( 1 + C_2 \left( \frac{W}{A} \right) n_{p\infty} \right) \right] = \beta (1 - \gamma)$$

The definition of  $\beta$  given above may be rewritten in terms of the adsorptivity,  $a$ ,  $a_i = \epsilon_i A_T / E_o$ ,  $i = 1, 2$

$$\beta = (a_1 - a_2) / (1 - a_2)$$

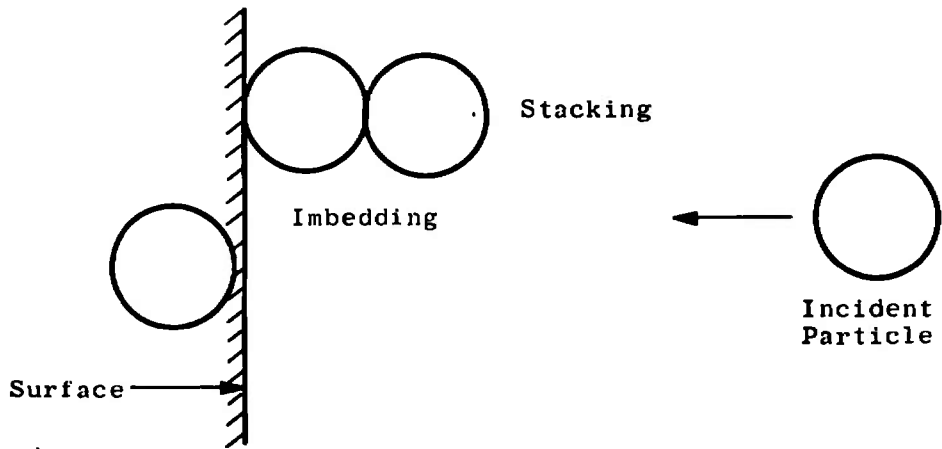
where  $a_1$  is the adsorptivity of the particles and  $a_2$  is the adsorptivity of the filter paper. If the particles are assumed to be carbon,  $a_1$  may be approximated by the adsorptivity of a rough deposit of lamp black, for which  $0.78 \leq a_1 \leq 0.84$  (Ref. 10). The adsorptivity of filter paper was 0.19. Therefore,  $\beta$  can be expected to vary in the range  $73.0 \leq \beta \leq 80.4$ . Hence,  $\beta < 100$  and  $\beta(1-\gamma) < 100$ , and the limiting value of SN  $< 100$ . That is SN is limited by the finite (non-zero) adsorptivity of the particles even though they completely cover the surface.

In the following discussion,  $\gamma$  was taken to be much less than 1.0. In order to check this approximation, several curves were examined using Eq. (IV-11). The two constants  $C_1$  and  $C_2$  were determined from curve fits, and the value of  $\beta(1-\gamma)$  was then evaluated from  $\beta = C_1/C_2$ . From these test cases,  $\beta(1-\gamma)$  was found to vary in the range  $73.0 \leq \beta \leq 80.4$ . Therefore, it was taken to be negligible, and for convenience in curve fitting,  $\beta = 76.7$  was used in all subsequent calculations. Typical values of SN versus W/A data used to evaluate SNR (the relative smoke numbers) are shown with the corresponding curve fits in Fig. IV-2. Data were also taken at values of W/A up to 0.21. Curve fits for these data are shown on Fig. IV-3. These figures (Figs. IV-2 and IV-3) illustrate that

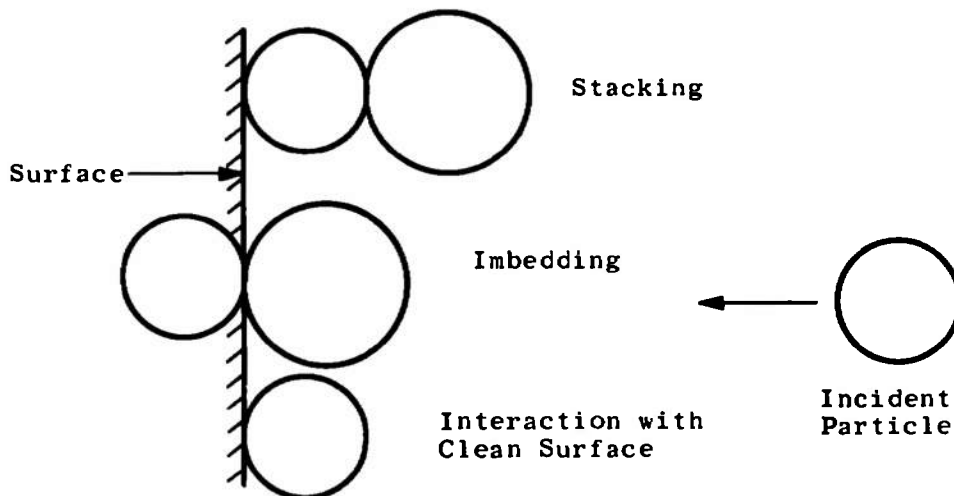
Eq. (IV-11) is capable of fitting the smoke number data over a wide range of  $W/A$ . Hash marks on the abscissa indicate the upper limit of  $W/A$  according to Ref. 4. The dashed lines on the figure indicate the least-squares curve fit to a straight line and are shown to provide a comparison between the methods. Wide variations between the two methods are seen to be possible.

The variation of the number density can be determined by solving Eq. (IV-11) for  $n_{p_{\infty}}$ . Figure IV-4 shows plots of the  $n_{p_{\infty}}$  values. The curves were normalized to centerline values to eliminate the currently undetermined constant  $\alpha_0 \mu_1$ . Observe that these results tend to vary more uniformly than the normalized SNR data. For these data,  $n_{p_{\infty}}$  values were obtained at  $W/A = 0.023$ .

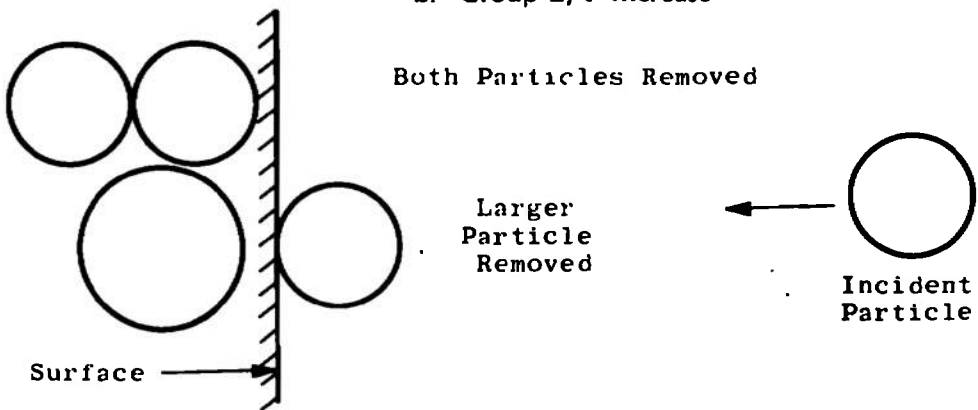
Unfortunately, time did not permit the complete reduction of the data in terms of  $n_{p_{\infty}}$ . However, these initial results indicate that more effort should be spent in improving the proposed analytical techniques.



a. Group 1, No  $\theta$  Change



b. Group 2,  $\theta$  Increase



c. Group 3,  $\theta$  Decrease

Fig. IV-1 The Three Surface-Particle Interaction Groups

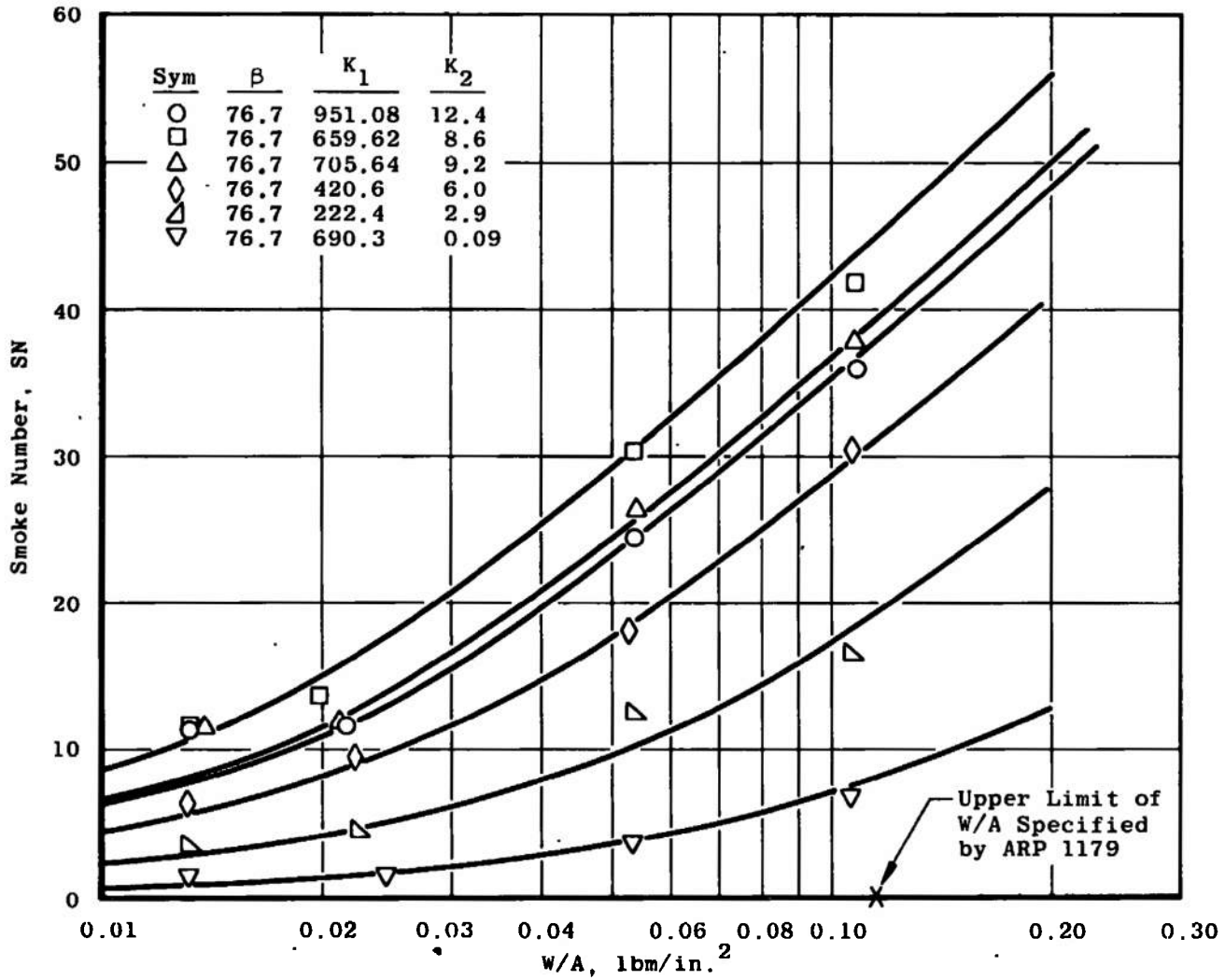


Fig. IV-2 Curve Fit of Typical SN versus W/A Data

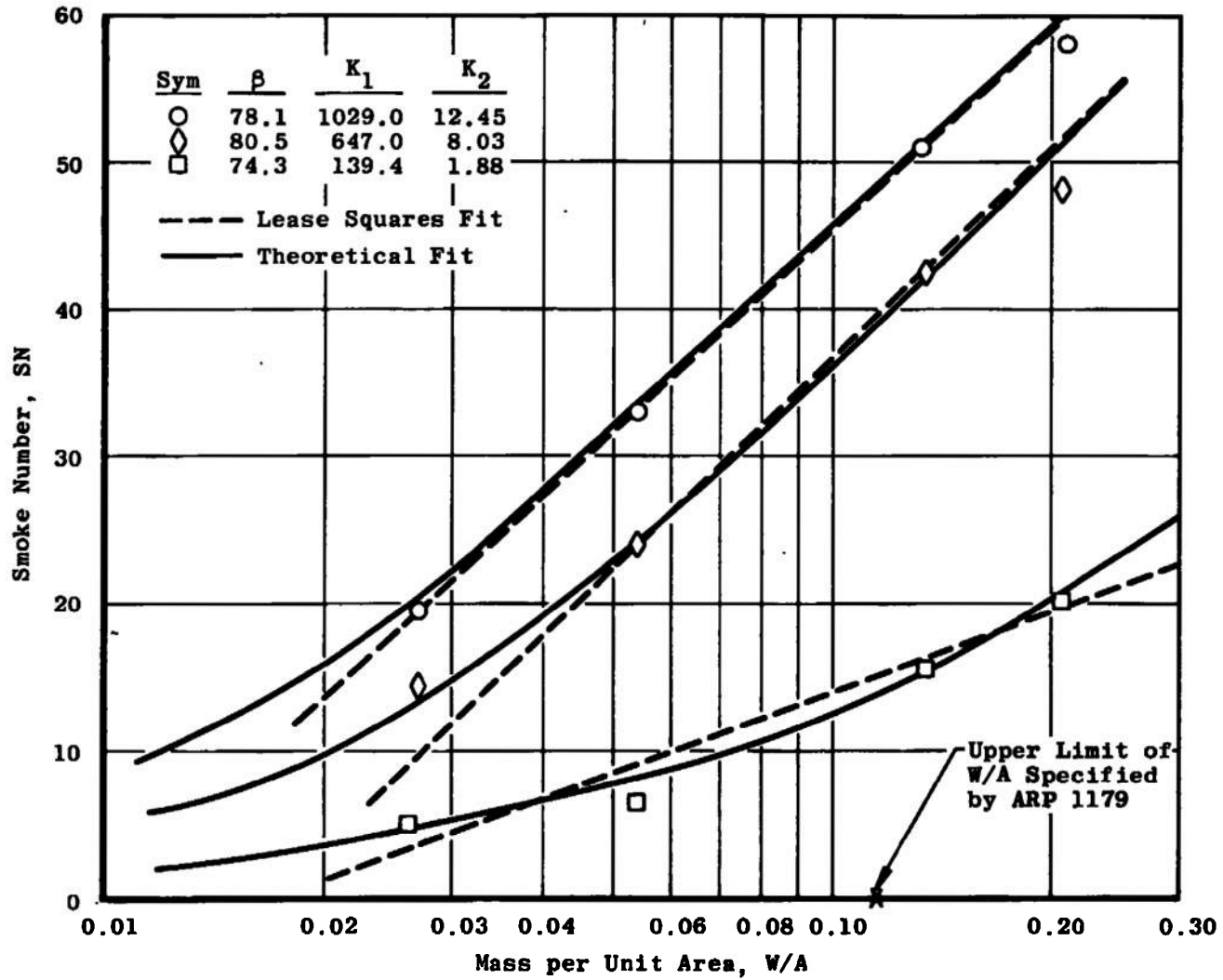


Fig. IV-3 Comparison of Linear and Theoretical Curve Fits

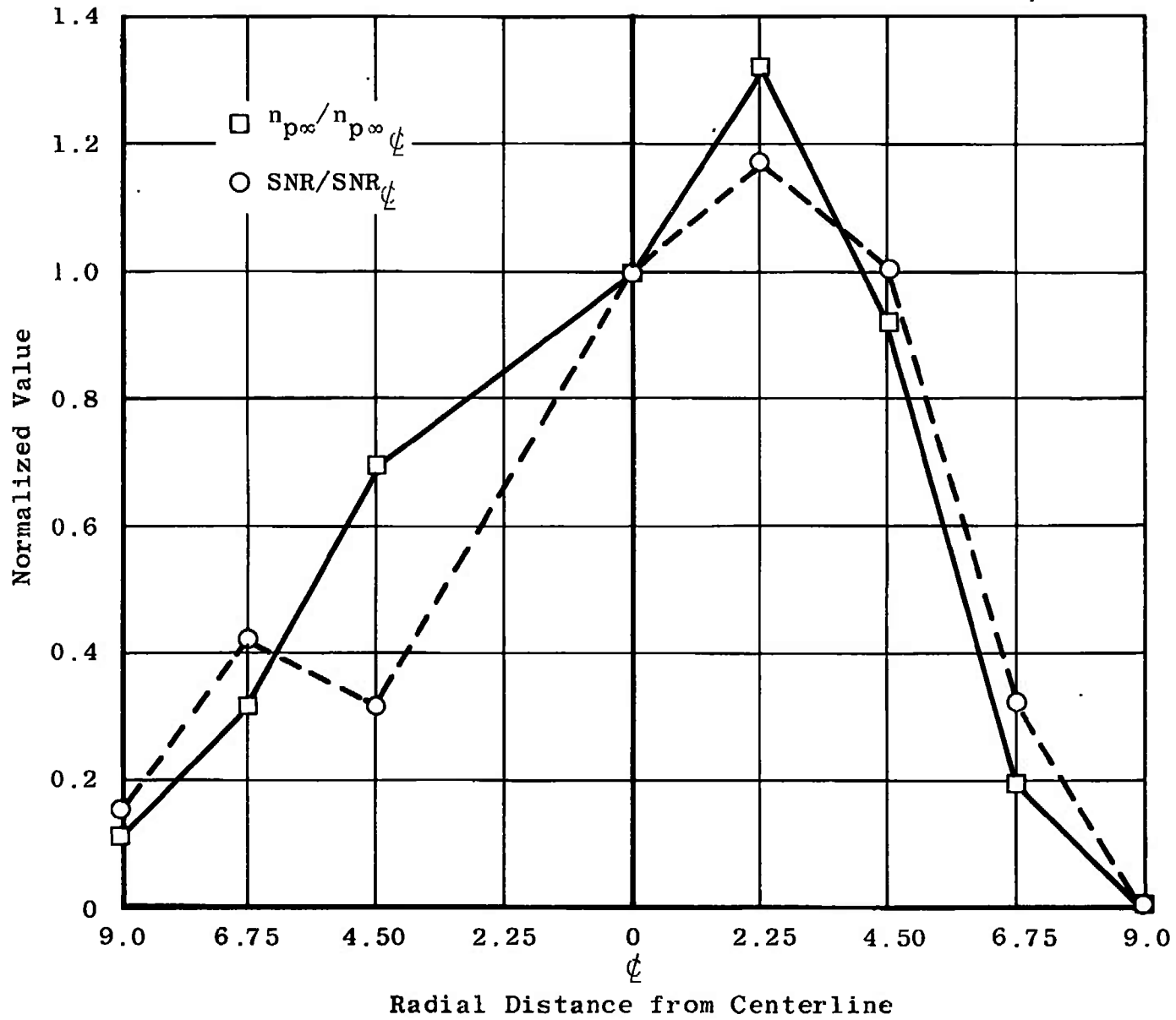


Fig. IV-4 Comparison of Normalized Relative Smoke Number with Normalized  $n_{p\infty}$

## DOCUMENT CONTROL DATA - R &amp; D

(Security classification of title, body of abstract and indexing annotation must be entered when the overall report is classified)

1. ORIGINATING ACTIVITY (Corporate author) Arnold Engineering Development Center, Arnol Air Force Station, Tennessee 37389		2a. REPORT SECURITY CLASSIFICATION <b>UNCLASSIFIED</b>	
		2b. GROUP N/A	
3. REPORT TITLE MEASUREMENT OF POLLUTANT EMISSIONS FROM AN AFTERBURNING TURBOJET ENGINE AT GROUND LEVEL PART I PARTICULATE EMISSIONS			
4. DESCRIPTIVE NOTES (Type of report and inclusive dates) March 23 to May 13, 1971--Final Report			
5. AUTHOR(S) (First name, middle initial, last name) J. W. Gearhart and J. A. Benek, ARO, Inc.			
6. REPORT DATE June 1972		7a. TOTAL NO OF PAGES 52	7b. NO OF REFS 11
8a. CONTRACT OR GRANT NO		9a. ORIGINATOR'S REPORT NUMBER(S) AEDC-TR-72-64	
b. PROJECT NO. 3066		9b. OTHER REPORT NO(S) (Any other numbers that may be assigned this report) ARO-ETF-TR-72-29	
c. Program Element 62203F			
d.			
10. DISTRIBUTION STATEMENT Approved for public release; distribution unlimited.			
11. SUPPLEMENTARY NOTES Available in DDC		12. SPONSORING MILITARY ACTIVITY AFAPL/TBC Wright-Patterson Air Force Base Ohio 45433	
13. ABSTRACT Smoke emissions were measured in general accordance with the methods specified in the Society of Automotove Engineers Aerospace Recommended Practice 1179. Measurements were made from 1 in. to 32 ft aft of the nozzle exit along the engine centerline, and both horizontally and vertically across the exhaust plume. The J85-GE-5 turbojet engine was operated over a power range from idle to maximum afterburning. The effects of inlet temperature and humidity on smoke production were determined, and trends of smoke production versus power setting were established.			

14.

KEY WORDS

LINK A

LINK B

LINK C

ROLE

WT

ROLE

WT

ROLE

WT

air polution  
air pollution  
contaminants  
turbojet engines  
particles  
emission  
exhaust gases  
exhaust emissions  
afterburner